PHOTOVOLTAIC PROCESS DEVELOPMENT AND INNOVATIVE TECHNIQUES

Author

FURRUKH ISMAIL
850810-T311

Supervisor

Björn Sohlberg
School of Electrical Engineering Hogskolan Dalarna

DEPARTMENT OF ELECTRICAL ENGINEERING
Hogskolan Dalarna
Borlange, Sweden.
08/2011

PHOTOVOLTAIC PROCESS DEVELOPMENT AND INNOVATIVE TECHNIQUES

Author

FURRUKH ISMAIL

850810-T311

A thesis submitted in fulfillment of the requirements for the degree of

M.S. Electrical Engineering

Thesis External Supervisor:

M. Khawar Ayub
AE(EM&P) Energy Management & Performance
TNB Liberty Power LTD, Mirpur Mathelo, Pakistan.

ABSTRACT

Photovoltaic processing is one of the processes that have significance in semiconductor process line. It is complicated due to the no. of elements involved that directly or indirectly affect the processing and final yield. So mathematically or empirically we can't say assertively about the results specially related with diffusion, antireflective coating and impurity poisoning. Here I have experimented and collected data on the mono-crystal silicon wafers with varying properties and outputs. Then by using neural network with available experimental data output required can be estimated which is further tested by the test data for authenticity. One can say that it's a kind of process simulation with varying input of raw wafers to get desired yield of photovoltaic mono-crystal cells.

Keywords:

Photovoltaic, Mono-crystal, Diffusion.

UNDERTAKING

I certify that research work titled "*Photovoltaic Process Development and Innovative Techniques*" is my own work. The work has not been presented elsewhere for assessment. Where material has been used from other sources it has been properly acknowledged / referred.

Furrukh Ismail

850810-T311

ACKNOWLEDGEMENTS

In the name of Allah who has all powers and provided me the ability to admire the beauties of knowledge through his blessings.

I am very thankful for my most respected and honorable supervisor, M. Khawar Ayub, and for Prof. Dr. Mohammad Ahmed Choudhry for providing me the opportunity to learn and benefit from his diverse experience and guiding me throughout my thesis work.

I also thank to IC Semiconductors (pvt.) ltd. for providing me opportunity to get my experimentation done by using costly raw material.

I am short of words to say thanks for the prayers of my mother which are enormous and source of my success through every walk of life.

Last but not least I want to appreciate the cooperation my wife showed that encouraged me to accomplish my work successfully.

TABLE OF CONTENTS

LIST OF FIGURES

Number *Page*

LIST OF TABLES

Number *Page*

CHAPTER 1

Introduction

1.1 Problem Statement

Photovoltaic processing is one of the most important emerging technologies to provide us with alternate source for our daily energy needs. In this thesis I have described the important aspects of processing that were experimented and innovated by efforts with limited knowledge & raw experimentation. It would have been much more beneficial to design the experiment and implement the logical flow of information to get the results based on assumptions. But here we used the symptom approach as after much experimentation we get to know by analysis of what to do next and where should we focus on in our single layer processing mechanism. After experimentation and process line behavior analysis the production line was set to provide us the required quantity of output.

By putting so much time and effort the thing that can be learnt with so much expensive experimentation is that we can put it in simple mould of Neural Network that can help us to describe the expected output of experimentation rather than actual experimentation involving manpower, energy, time and money.

Reason and justification of my work is creating a simulator based on the experimentation that can generate results resembling actual experiments without performing actual expensive experimentation.

Aims & Objectives

Following are the main aims and objectives

- This research work is to provide the complete understanding of FAB (Fabrication Area) to provide some exposure of semiconductor industry.
- It is also focused in designing some simulation application related to photovoltaic processing that yield results before the actual experimentation be performed for the required field.
- This study also helps as platform for the future improvements and modification of photovoltaic process by adding some software helping tools of Neural Network.

1.2 organization of Thesis

Organization of this thesis is as under:

Chapter 2 presents the literature review with all the concerned components of fabrication process & relevant research papers for each segment.

Chapter 3 describes the process variables of photovoltaic processing with all the elements including material, machine, environment and software.

Chapter 4 expresses the experimentation and results covering all aspects of my work.

Chapter 5 talks about the futuristic and methods to improve the working in photovoltaic's by adding efficiency and delicacy through supported software simulators.

CHAPTER 2

Literature Review

Photovoltaic processing has several aspects that can be discussed under:

1- The physical process involved in making solar modules, raw materials that include silicon wafers, processed water and air for fabrication area, multi-stage diffusion furnaces for doping of N-type layer, anti-reflective coatings, edge-isolation, surface texturing, back surface field and front metallization.

2- Other aspect is concerned with the testing and measurements of sheet resistance to probe into diffusion pattern/concentration, current and voltage measurements to determine efficiency for improvement.

3- By experimentation and simulation we can get the neural network trained to help us predict the outcomes and alert us for any change induced in during processing.

So following aspects of process are important for better understanding of PV process and its variables:

2.1 Process Description of DI water-Application in Semiconductor Industry:

This part of literature gives some layout of design that helped to understand the DI water production from manufacturer's point of view that was used for process applications. The raw water is taken from well and processed through sand filters to remove the particles. After sand filters water was put to carbon filters to remove the biological impurities that can pollute the quality of water. Reverse osmosis is then performed and after that the heart of the DI process comes, ion exchange bed that purifies the water with ion

exchanging. Water is then passed to the UV light for the killing of bacteria and making it semiconductor grade water for FAB applications. The water is continuously run to make it pure from the unnecessary growth of bacteria and filtering the contaminants in piping & pumps. About 18MΩ resistance water is use d for semiconductor applications as aggressive cleaning agent.[1]

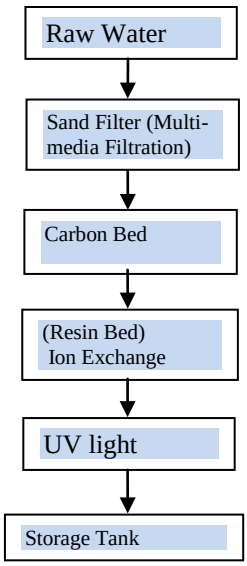

Fig 2.1: DI water plant layout.

2.2 DIFFUSION

The diffusion process is expressed in-depth with the evaluation of diffusion length specially for different ramp times.

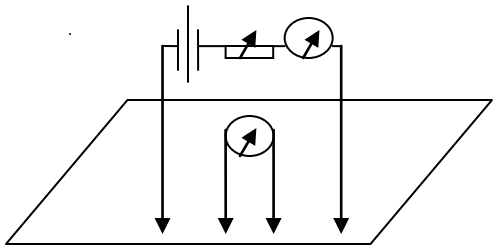
Fig.2.2- Four Point Probe

The addition of phosphine as dopant on boron doped silicon solar base material is key component of solar process development. The temperature profile of the recipe synthesis is fine tuned on the basis of calculation, experimental results for the fabrication line & by the help of supporting study. The sheet resistance measurement in my experimentation is performed by 4-point probe (ResMap) whose introductory knowledge can be referred by this article to get the spread of doping.[2]

2.2.1 Diffusion with varying impurity

Diffusion process is studied on a surface of constant concentration with varying impurity concentration. The doping profile at low concentration takes the form of $C = C_s' erfc(x/2\sqrt{D_l t})$ where D_l is the diffusion coefficient at low impurity concentration, while C_s is the apparent surface concentration depends on the actual surface concentration and also depends on how the diffusion coefficient varies with impurity concentration at high concentrations. It is a constant for a given diffusion system but could be orders of magnitude higher than the actual surface concentration. Empirical data shows the boron and phosphorous diffusions in silicon are according to the predicted function. However as the concentration raises from $10^{20}\,cm^{-3}$ then the diffusion constant is a strong function. As there is no theory available to calculate the concentration profile so its difficult work for those who are engaged in making and designing the semiconductor devices at high concentration diffusions.[3]

2.2.2 Sheet Resistance Measurement

The Four-Point Probe can be used to measure film thickness, but is usually used to measure the sheet resistance of shallow layers (as a result of epitaxy, ion-implant,

diffusion or sputtering) and the bulk resistivity of bare wafers. The schematic representation of the Four-Point Probe is shown in Figure 1. The theory behind this is a fixed current is injected into the wafer through the two outer probes, and a voltage is measured between the two inner probes. If probes with uniform spacing *s* are placed on an infinite slab material, then the resistivity, ρ, is given by

$\rho = 2\pi s V/I$ μOhm-Centimeters for $t>>s$

and

$\rho = (\pi t/\ln 2)V/I$ μOhm-Centimeters for $s>>t$,

with *t* representing the thickness of the thin film. For shallow layers, the above equation gives the sheet resistance as

$Rs = \rho/t=(\pi t/\ln 2)V/I=4.53V/I$ μOhm-Centimeter for $s>>t$.

The approximation used in the above eq. is easily met for shallow layers in silicon.[4]

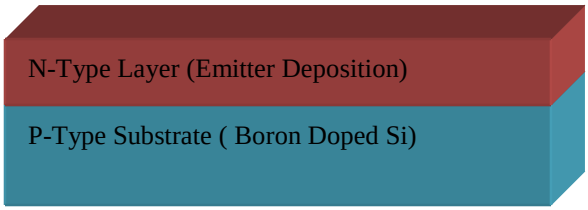

Figure: 2.3 Top Layer Sheet Resistance Measurements.

2.3 Surface texturing:

It is well observed that the surface texturing is helpful in improving radiance and surface area to increase output of solar modules. It is helpful in giving the SEM-scanning electron microscope image of the surface textured. As per procedure to dip the silicon in KOH solution after deglazing & RCA cleaning for 10 minutes.

Initially the wafers are boiled for five minutes in acetone solution to remove the grease and washed in ethanol. Sawing defects are countered by NaOH solution after which the wafers are dipped in HF solution to remove the native oxide.

The pyramids formed due to etching are determined by temperature and time profile maintaining. The best results can be established by using the concentrated KOH solution at 95°C for 10 min. , and the pyramids are uniformly distributed with size under 4 micron. After the surface texturing area of impact is increased to help by improving the efficiency of cell with low reflectance. The textured solar cell gives us the high output relative to the not textured solar cells. The typical surface image for the process is shown as under:[5].

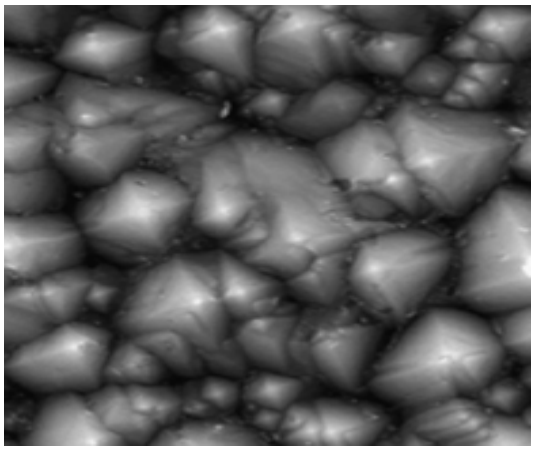

Figure 2.4: Pyramid Surface Texturing.

2.4 Techniques to Improve Manufacturing Process:

Manufacturing innovations are with the inclusion of step by step process improvement for the maximum yield and efficiency.

This paper helped to inculcate the thought process involved in improving the production of solar cells and their efficiency that provided a pattern to study streamlined data and processing steps as depicted in figure.[6]

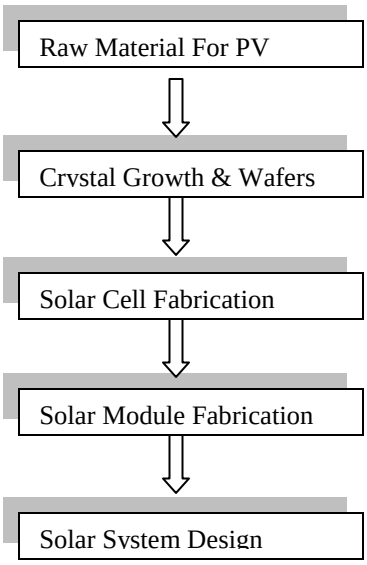

Figure 2.5: PV Product Flow.

The decrease of minority-carrier lifetime with resistivity and with illumination level in bifacial dendritic web silicon solar cells is addressed. This variation of lifetime is shown to be consistent with the presence of a distribution of defect levels in the band-gap that arise from extended defects in the web material. The extended defects are precipitates, recently shown to be oxide precipitates that decorate dislocation cores. It follows that the sensitivity to this background distribution of defect levels increases with doping because the Fermi level moves closer to the majority-carrier band edge. It is not necessary that doping atom itself, or a complex including the doping atom, acts as a recombination center in order to explain the observed decrease in lifetime with doping density. Good agreement is obtained between calculated and measured values of short-circuit current and quantum efficiency for bifacial cells covering a range of doping density (6 x lOI4 to 3 x 10l6 ~ m - a~nd) illumination level (0.001 to 1 sun), with illumination from either back or front of the cell. The implications of this approach extend to concentrator cells and to other devices in which minority-carrier lifetime is an important parameter.

This includes devices made using Czochralski-grown silicon, where oxygen and oxide precipitates likewise play an important role in determining lifetime.[7]

Table: 2.1 Chemical Etchants for Silicon Defects.[19]

<100>/<111>	Vol. Composition			Approx. Etch Time (Min.)
Ingot or substrate	49% HF	.75M CrO_3	H_2O	
n or p >.2Ω-cm	2	1		5
p-type<.2Ω-cm	2	1	1.5	5
n-type<.2Ω-cm	2	1	1.5	10
Oxidized Wafers	2	1		1 to 2

The measured short-circuit current density in bifacial dendrite web silicon solar cells has been found to decrease with decreasing base resistivity, particularly under back illumination. In addition, the ratio of short-circuit current under back illumination to short-circuit current under front illumination was observed to vary with light intensity. These observations reflect the fact that the minority carrier lifetime in the base of these cells is a function of the base resistivity and the illumination level. The dopant was assumed to play only an indirect role in determining lifetime. The formation of electrically active complexes involving the dopant atom are not thought to be a significant factor in explaining the observed decrease in lifetime as the doping density increases because DLTS measurements on web cells have failed to indicate any systematic discrete deep levels even for depths up to 60 pm. Instead, this decrease in lifetime is shown to follow from a distribution of defect levels in the band-gap. These levels are a consequence of extended defects that have been observed in the web material. The extended defects are oxide precipitates and the dislocation cores that they decorate. The dopant, then acts only in the indirect role of moving the Fermi level over an existing

background distribution of defect levels that arise from the extended defects. **A** parabolic distribution of defect levels in the band-gap was assumed and minority-carrier lifetime was calculated as a function of doping density and excess carrier concentration (illumination level) using the Shockley- Read-Hall theory. The short-circuit current densities that were calculated using these lifetimes agreed reasonably well with measured values for bifacial dendritic web silicon solar cells. The measurements were made over a range of doping densities (6 x 1014 to 3 x 10l6 (31-r~) ~ and illumination levels (0.001 to 1 sun) for both front and back illumination of the bifacial cells. The qualitative agreement over a variety of conditions that results from a single choice of defect level distribution lends credibility to this approach.[7]

2.5 Neural network selection-Reason justified:

Neural network based approach is used to predict the wafer yield in IC manufacturing. With this approach computer software can be written to accurately predict the wafer yield in IC manufacturing. In this paper small defect approximately the size of transistor are being studied rather than those often occur due to mishandling of wafers. Basically these small defects are due to clusters and for that unsupervised neural network approach is used. ART adaption resonance theory, the degree of similarity between new and old pattern is defined by vigilance parameter (L). ART has several variations, here the Fuzzy ART is being used which consists of two layers.

1) Input (F1) layer
2) Output (F2) layer.

And three parameters

1) Choice parameter $\alpha>0$;

2) The learning rate $\beta \in [0,1]$;

3) Vigilance parameter $\rho \in [0,1]$.

These parameters are specified by the user. The approach define that (x_i , y_i) are the coordinate of the defect map on wafer. Then their scale between min:max value is defined by ui and vi as

$$u_i = \{x_i - \min(x)\}/\max(x) - \min(x) \text{ ----------(1)}$$

$$v_i = \{y_i - \min(y)\}/\max(y) - \min(y) \text{ ----------(2)}$$

the explained approach is used to identify the defective wafers and tested in FAB. This approach could also be used in LCD & PCB production lines as well. [8].

2.5.2 Neural Network Model with data limitations

A special artificial neural network (ANN) method discussed to develop satisfactory models even though fewer experimental data exist than there are coefficients in the ANN models. The method aims at constructing a model which can satisfy the criteria of minimum training error, maximum smoothness, and simplest network structure. Two ANN models were developed for a plasma etching reactor using $CF_4/0_2$ or CF_4/H_2 as a reactant that relate the manipulated and controlled variables or the manipulated and performance variables, respectively. Comparison of the predictions made by the ANN'S with those made by the second order regression models that were used as the basis of the experimental design to get the data indicated that the ANN'S predicted the process behavior more reasonably than the classical regression models when the process is operated at various operating conditions.

The development of reliable models is the key to the investigation of process behavior and the realization of real time control of a highly nonlinear multi-input multi-output

plasma etching process. One difficulty often encountered in developing a plasma etching model is the lack of sufficient experimental data. Here artificial neural networks (ANN'S) have been used as empirical models for the plasma etching process. To ensure valid generalization (prediction) capability of models derived from limited data, a method based on a modified predicted squared error (MPSE) criterion has been introduced. This method aims at identifying the tradeoffs among the most promising ANN models so that the model selected provides a balance between the lowest prediction error, the smoothest prediction, and the simplest model topology. Using this method, ANN models were developed for a plasma etching process using $CF_4/0_2$ and CF_4/H_2 as reactants. The simulation results showed that the ANN'S predicted the process behavior more satisfactorily than regression models both at the normal operating conditions and at the upper or lower limits of the operating range.[9]

2.6 Random data and use of neural network:

Supervised learning method can be used in which error is minimized using the gradient descent approach , weights are adjusted in such a way as to minimize the overall system error.Application is on the PECVD silicon nitride films which is used as ARC (anti reflective coating) on the solar cells. Neural network used to develop and obtain accurate , useful manufacturing models for the PECVD of silicon nitride films. Experimentation was done using the plasma therm-700 series batch reactor operating at 13.56 MHz using NH_3 ammonia ,silane SiH_4 and nitrogen as feed gases. Deposition was varied and positive charge concentration was obtained using C-V measurements. Effective life time was measured using photoconductive decay (PCD) tester. Neural network has emerged as attractive alternative because of its ability to map the non-linear complex trends due to

self organizing capability & adjusting the weights / connection strengths. Error is minimized using a gradient descent method in which weights are adjusted accordingly. Neural model is optimized using a Nelder-Mead simplex search algorithm. PECVD silicon nitride films have been modeled using optimized back-propagation neural networks ,that determine the optimal process condition to grow nitride film and also can be used as effective tool in enhancing the effective lifetime with low sheet resistance.[10].

2.6.1 Characterization through NN

Deposition of silicon nitride (SiN) film is one of the most critical processes that determine the efficiency of solar cells.

Qualities of SiN film deposited by plasma enhanced chemical vapor deposition depend on many process parameters. Predicting film properties is very important to their optimization as well as to gain insight into underlying deposition mechanisms. For plasma-driven processes, however, it has been a difficult task to construct prediction models due to complexity within a plasma. In this study, a predictive model for a SiN PECVD process was constructed and used to understand physical deposition mechanisms. The interpretation was mainly focused on the refractive index, particularly with respect to the substrate temperature. SiN films investigated were deposited in a Plasma-Therm700 series batch reactor operating at 13.56 MHz. The process was characterized by a central composite circumscribed, experimental design, consisted of Z"-'fractional experiment and **12** axial points. The process parameters that were varied in the design include **a** radio frequency power, pressure, substrate temperature and three gases *(Silane ,* NH_3, and N_2). One center point was also added. Resulting **32**

experiments including one center point were used to train a neural network. Prediction performance of trained network was then tested with the additional 12 experiments. Three-inch, float zone p-type silicon wafers, with (100) orientation and a resistivity of **2.0** R-cm, were used as the substrates. During the deposition, SiH_4 was diluted to 2% in nitrogen. Approximately 0.05 pm silicon nitride was deposited. Refractive index to be modeled was measured by a helium-neon laser having a wavelength of **6328.** As a modeler, a back propagation neural network (BPNN) was used. The training factors involved in BPNN training were optimized. The root mean-squared prediction error of the optimized model is 0.018 compared to previously constructed models, the model demonstrated much improved prediction. From the optimized model, various interactions between the substrate temperature and the other process parameters were predicted and interpreted on the basis of the linear dependency of the refractive index on the SiH/NH ratio. The refractive index increased with increasing the SiH_4 flow rate or the substrate temperature. In contrast, increasing N_2 decreased the refractive index. Meanwhile, the refractive index behaved independently of the RF power. The interactions were very complex **as** the substrate temperature varied particularly at either high SiH4 flow rate or low RF power.[11]

2.7 Why back-propagation NN is used:

Neural network has been used to model PECVD process .The SiO_2 deposition was characterized via 2^{5-1} fraction factorial experiments. And data from this experiment was used to train feed forward neural network using the error back propagation algorithm. Optimal neural network structure and learning parameters were determined using second fractional factorial experiment.

In development of the neural model output responses : deposition rate , refractive index , permittivity , film stress , wet etch rate , silane concentration and water concentration were used. Feed forward neural network were trained using error back propagation algorithm & we refer it as feed forward error back propagation (FFEBP) network.

SiO_2 growth was done by PECVD system at 13.56MHz with electrode spacing of 2.29cm.Metrion 2010Prism used to determine thickness, Flexin F2320 was used to measure the radius of curvature.

NN has capacity of learning non-linear arbitrary mapping between noisy set of input and outputs, activation function used is sigmoid : $y = 1/ 1+e^{-x}$ which provide the added degree of freedom not available in statistical regression techniques. FFEBP is a supervised learning method .Error is minimized using gradient descent approach .Performance of FFEBP depends upon learning rate , momentum and training tolerance. Performance index for each seven PECVD outputs were as $PI=K1\sigma^2_t + K2\sigma^2_p$ where k1=1,k2=10.

Optimization of neural process model was done by Nelder-Mead simplex algorithm to minimize the performance index itself. The PECVD process was characterized by varying the five controllable parameters in a fractional factorial design. FFEBP neural network were trained and later optimized to predict seven key PECVD output responses.[12]

2.8 Real time decision making a reason for NN use:

Multilayer preceptor neural network is used for various applications in semiconductor industry manufacturing. As the complexity and non-linearity make experimental data expensive to get , so neural network as tool help in IC-CIM. In this paper the feed forward error back propagation network is developed with genetic algorithm and thus

used to assist the semiconductor process. In ObOr NNS developed in JAVA. It is platform independent and can be used on most operating system. Using the error back propagation training algorithm ObOrNNS yield excellent results and the java implementation enables ObOrNNS to be customized with minimum effort .It allows the hybrid neural network for semiconductor experimental modeling and parameter prediction with genetic algorithm provided recipe synthesis using trained neural net. Models in ObOrNNS can conceivably be used for real time control of semiconductor fabrication equipment. By integrating process modeling optimization and control ObOrNNs can contribute to the success of semiconductor manufacturing in an automated & efficient manner.[13]

2.9 NN specifically recommended for wafer fabrication/ process :

Predictor model is formed using the neural network & statistical response surface techniques for the chemical vapor deposition (CVD) silicon epitaxial process. Prediction performance of neural network is better than the linear and quadratic response surface models. Neural network model is more accurate with the increasing complexity and also help to determine the critical parameters in processing. It also help when used in reverse to determine the parameters of a recipe for a process.

In this process the infrared heated barrel reactor is used to deposit the high quality epitaxial layer of doped silicon substrates for the production of bipolar and MOS integrated circuits. Mixture of gases enter the bell jar surrounded by infrared and exit from the hole in the bottom , important is the uniformity of layer that is deposited in this process on the silicon with deposition rate of 1 micron/minute. Convective transport in the barrel shows the deposition parameters to be effective depending upon the orientation

parameters jetx, jety, bmvl, bmvr, H2m, H2r. Thickness measurement is done at five points on the wafers. The input parameter setting was varied according to a central composite design consisting of 2^{6-1} two level factorial design (32 runs) combined with 9 replicated runs and one at a time large offset of each of six parameters in both directions 12 runs. In this experiment a part of the data is used to train the neural network and rest is used to test the NN.

In this experimental model the feed forward error back propagation network is used with one hidden layer of nodes. The choice of single hidden layer was dictated by indirect relationship of the control parameters and the output observation with the physical and chemical properties of the process related to the input parameters and the output variables. In network the inputs were normalized between -1.0 and 1.0 .The transfer function at each node in the hidden and the output layer was chosen as tanh (y),where the sum of the inputs into the node from the previous layer .The network input from the layer k into a node layer j is given by:

$$y_j=\sum_k W_{jk}\, U_k$$

U_k are the outputs from the nodes in the previous layer k and W_{jk} are the respective weights for the connections from these nodes. Therefore the output of the same node in layer j is given by

$$V_j= \tanh(y_j)= \tanh(\sum_k W_{jk}U_k)$$

The network was trained by back propagating the error using the generalized cumulative data rule. The inputs were chosen at the random from the training data set .The training was performed for approximately 6000 iterations. Also the model of inverse neural network was developed to determine the process control parameters when a specific

output is required .Also by this model it came to know the jety variable was not that significant in prediction of thickness which was also confirmed by the engineers knowledgeable in this process.

So in this paper the predictor models generated and statistical response surface techniques for the CVD silicon epitaxial process. The prediction of neural network is better in the complex processes in real time applications also the inverse model is used to predict the significant parameters to get the required outputs by varying the input significant for the process variables.

By this study we can also propose the inverse network model of the process as part of an adaptive feedback controller which would also be effective in a non-linear environment.[14]

2.10 Analysis using neural network as effective tool:

Low resistivity of 0.2-0.3 Ω.cm is optimum for high quality single crystal silicon for solar cells. However for the cast mc-Si, this optimum resistivity increases owing to a doping defect interaction. Which reduces the bulk lifetime at the lower resistivity, Solar cell fabrication on a 175μm thick, 1.5Ω.cm wafer showed no appreciable loss in the performance of cell when compared to the 225μm thick cells. The cost of PV generated electricity must be many folds less to get into comparison with the electricity provided by utility as using the low cost mc-Si material with less thickness can make the step toward cheaper solar cells also the SP method to lower the cost of processing. The quality of wafer depends on its location in the mc-Si ingot.

In this paper the solar cell with SP contacts and from four different ingot of boron doped P-type material were fabricated using the standard RCA cleaning and $POCl_3$ diffusion to

form a 45Ω/sq n^+ emitter followed by the low frequency PECVD SiN_x antireflection (AR) coating deposition on front. Samples were obtained by after Al screen printing on back and Ag grid printing on the front. Then the cells were co-fired in IR belt furnace forming the Al-BSF and Ag front grid. Cells were then annealed in forming gas at 400ºC before IV measurement wafers with 225µm and 175µm. It was evident from the experimentation that the wafers with 175µm thickness have 16.4 ~ 16.7 % efficiency and there is no such dependence on the resistivity. So experimentally it is evident that the increased doping does not guarantee increase in performance. Open circuit voltage increase was observed with increasing resistivity. We can say that the device modeling optimally performed with lower thickness and lower resistivity also we can link the doping defect interaction with increasing the optimum base resistivity to higher values.[15]

2.11 Efficiency improvement of silicon solar cells.

Efficiency of solar modules can be simply considered as ratio of energy impact on its surface and its conversion to electrical output keeping air mass density in view. There may be different ways to measure the efficiency based on time and need.

2.11.1 Ways to measure output of solar cells

The efficiency of a photovoltaic device is defined as the maximum power generated Pm divided by the product of the input irradiance and its area. This conversion efficiency depends on many factors, such as irradiation and temperature. The manufacture processes usually cause differences in electrical parameters, even in cells of the same type. Moreover, if the losses due to cell connections in a module are taken into account, it is

difficult to find two identical photovoltaic modules. Therefore, only the experimental measurement of the I-V curve allows us to know with precision the electrical parameters of a photovoltaic device. This measure provides very relevant information for the design, Installation and maintenance of PV systems. Given the large number of methods for I-V measurement, a survey of them would be very beneficial to researchers in PV systems.[16]. Following methods of solar module characteristic finding are here:

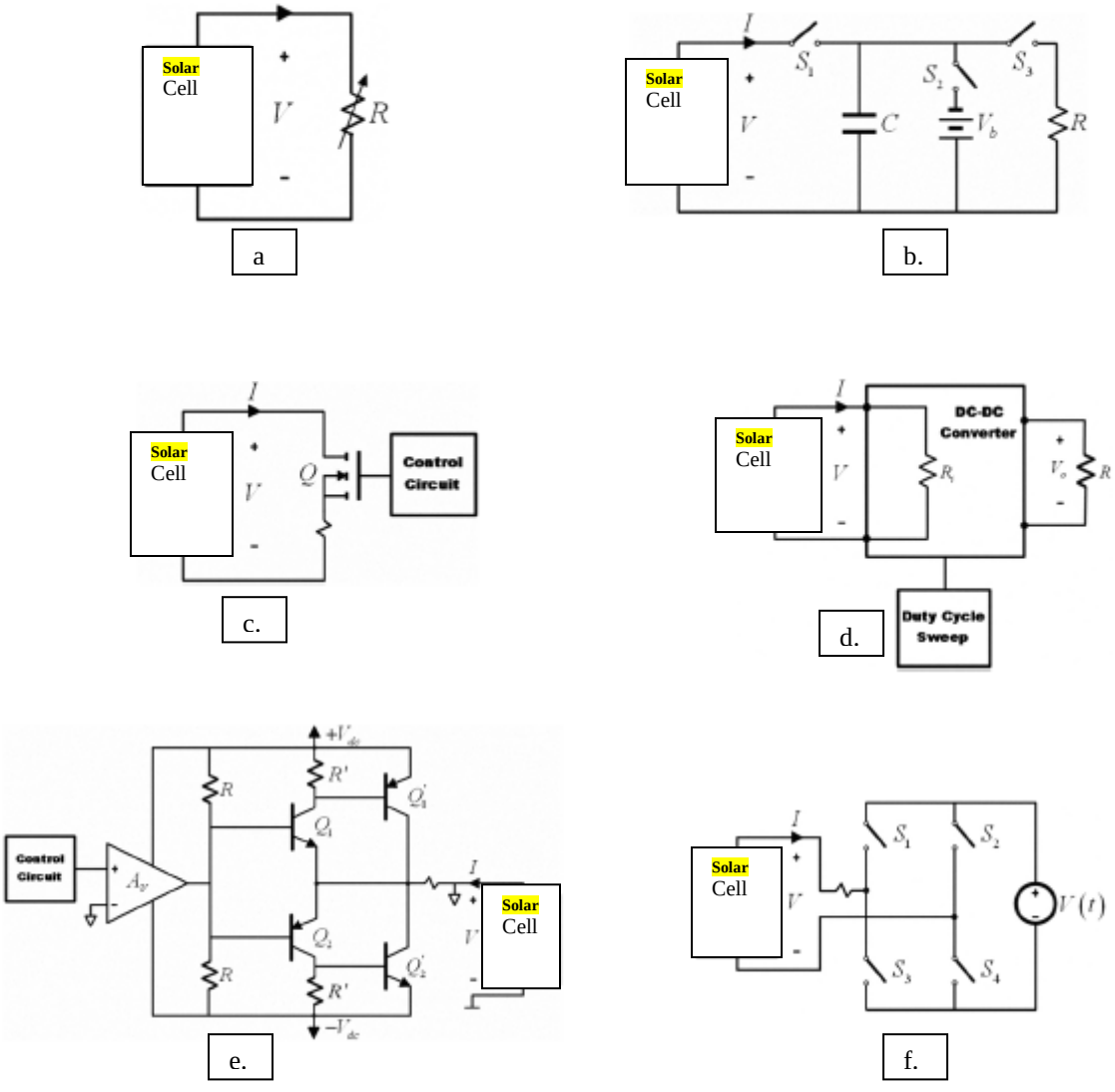

Figure-2.6: a-Variable resistor, b-Capacitive load, c-Electronic load, d-DC-DC convertor load, e-Bipolar power amplifier, f-Four Quadrant power supply

Table-2.2: Solar Module Response

	Flexibility	Modularity	Fidelity	Fast Response	Direct Display	Cost
Variable Resistor	Medium	Medium	Medium	Low	No	Low
Capacitive Load	Low	Low	Medium	Low	No	High
Electronic Load	High	High	Medium	Medium	Yes	High
Bipolar Power Amplifier	High	High	High	Medium	Yes	High
4-Quadrant Power Supply	Low	Low	High	High	Yes	High
DC-DC Converter	High	High	High	High	Yes	Low

2.11.2 Testing of solar cells for efficiency

Very High Efficiency Solar Cell (VHESC) program is developing integrated optical system-photovoltaic modules for portable applications that operate at greater than 50 percent efficiency. We are integrating the optical design with the solar cell design, and we have entered previously unoccupied design space. A test bed for rapid development and verification of performance of subsystems is also being developed. The results and analysis of the first complete integrated optics and solar cells on this test bed are reported. The demonstration has achieved efficiency greater than 36%. Analysis shows a direct path to efficiencies greater than 40%. These initial results have not been verified by NREL or any other 3rd party. We have previously reported the sum of the solar cell efficiencies to be over 42%, and optical subsystem efficiency greater than 93%. Our approach is driven by proven quantitative models for the solar cell design, the optical design and the integration of the two developing high-efficiency modules based on co-design of the optics, interconnects, and solar cells. The new architecture significantly increases the design space for high-performance photovoltaic modules in terms of materials, device structures, and manufacturing technology. It affords multiple benefits, including increased theoretical efficiency, new architectures that circumvent material/cost trade-offs, improved performance from non-ideal materials, device designs that can more closely approach ideal performance limits, reduced spectral mismatch losses, and

increased flexibility in material choices. An integrated optical/solar cell allows efficiency improvements while retaining low area costs and hence expands the applications for photovoltaic. The new design approach focuses first on performance, enabling the use of existing state-of-the-art photovoltaic technology to design high performance, low-cost, multiple-junction III-Vs for the high and low energy photons while circumventing existing cost drivers through novel solar cell architectures and optical elements.[17]

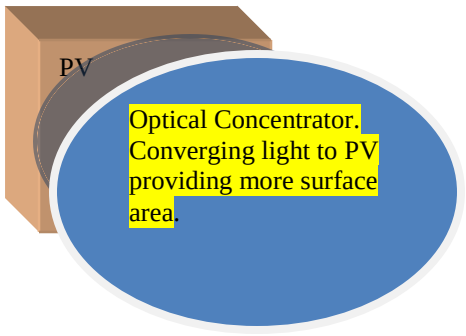

Figure-2.7: PV Optical Enhancement Application.

So these are some of the review that tells us about the diversity and depth of PV field and innovations in making good out of the alternate energy resources. Neural network also playing its vital part in enhancing the capability of PV processing through induction on intelligence.

CHAPTER 3

Process Variables

This research work is divided into following sections that include the material, machine, environment and software. Here some detail of semiconductor material, tools to fabricate solar cells as photovoltaic application, experimentation environment necessary for the processing and software application for result prediction will be provided.

3.1 PV Process Materials

- Semiconductor material used as base is silicon with melt growth crystal CZ (Czochralski) and FZ (float zone). The CZ is mostly used photovoltaic material in application for all the single crystal modules we use now days. Although the material cost is one of the crux that make the modules less feasible with respect to economy. Here we have mono-crystal CZ material at base which is P-type doped and having 110 crystal lattice orientations.
- Second material of choice is the semiconductor grade PH_3(phosphine) for N+ doping on the P-substrate and is here used as the only dopant with N2 providing oxygen free environment for the diffusion of emitter.
- In the processing of PV cells we are using KOH for surface texturing and RCA clean is done by the use of standard process which also include the consumption of HF+DI (1:10) to remove native oxide, 15 min $NH_4OH+H_2O_2$+DI (1:1:5) @50-70°C then DI (de-ionized water) rinse for 5min.
- Aluminum BSF (5072B) for back surface plating and Ag/Al (4075) for front grid contacts is used in this experimentation.

- IPA (isopropyl-alcohol) is used as general cleaning agent for vacuum wand and other applications.

3.2 PV Process Equipment

Here I have described the machines that were used during the experimentation of PV processing in each process step.

1- For the wafer rinsing and surface texturing I used the Teflon made sinks with their supporting features of vacuum wand and N2 drying. For quick wafer drying the spin rinse and dryer was used with 3000rpm speed.

2- Teflon cassettes were used to carry the wafers before diffusion and metal cassettes were used to carry them in metallization steps.

3- 3-Zone Bruce-7355 diffusion furnaces were used with accuracy of +/_ 1°C tolerance in temperature with temperature range up to 1200°C.

4- Silicon carbide boats were used to carry the wafers into the furnace with programmable movement and supported by baffle wafers at endings of each boat.

5- HEPA (high efficiency particulate air) filters were used to clean the class 10 clean rooms which also maintained the high pressure inside FAB. To help reduce particle impurities.

6- Ultrasonic hot bath was used to remove the BSF ash after 1Hr dip in concentrated HCL sinks.

7- 4-Point probe (Resmap) was used to take the sheet resistance of wafers at different stages to keep check of process stage and dopant concentration parameterization.

3.3 PV Process Environment

- HEPA (high efficiency particulate air) filters are used in fabrication area to help make it particle free and good for processing.
- Class 10 clean room was maintained to help reduce the impurity poisoning and metallization into the furnaces in order to get good yield.
- Bunny suits (clean room suits), face masks, powder free gloves, safety shields, safety goggles, clean-room wipes and shoe-masks were implemented to maintain the cleanliness.

3.4 PV Process Software Applications

1. 3-Zone Bruce diffusion furnaces have their 7355 microcontrollers installed that can be programmed through ladder logic according to the recipe for 1)Temperature 2)Gas Flow 3)Boat Movement and 4) Alarm point settings to successfully implement the emitter deposition steps and other processes. All these furnaces are connected to the central computer for programming and manual option is also available to troubleshoot for any problem in processing of feedback checking of mentioned parameters.
2. For sheet resistance of wafers the ResMap 4-point probe used its own inbuilt software that can take the reading in Ω/Sq. or in Ω.cm at designated points of 2-6 Inch wafers as mapped for process requirements.

3.4.1 Matlab - NNtools Application

Matlab7.6.0.324 (R2008a) is used to do the simulation on the results obtained from the experimentation to form the neural network.

Here we have used the input training data for network training and then checked the validity of the defined feed-forward backpropagation network.

The learning algorithm used are trainlm & traingd with graphical user interface of nntools showing the plotperform, plotregression, plotstate and network response figure for validation/checking of outputs.

The network for simulation has been defined with help of variable in data provided with experimentation and their outputs are incorporated to get the results for final checking.

3.5 Diffusion in Semiconductors

Diffusion is the travelling of electrons/holes from higher concentration toward lower concentration and we define diffusion constant for every charge state with different temperature dependencies.

We have

Table:3.1- activation energy, Q and D□ for diffusion by vacancy in silicon as

		Q(ev)	D□ (cm^2s^{-1})
Si	$V^{□}$	3.9	0.015
	V^{-}	4.54	16
	$V^{=}$	5.1	10
	V^{+}	5.1	1180
P	$V^{□}$	3.66	3.85
	V^{-}	4.0	4.44
	$V^{=}$	4.37	4.42

3.5.1 Diffusion of Phosphorous in Silicon

The diffusion of phosphorous in silicon can be viewed in this equation.

$D_p=hD_i°+D_i-(n/n_i)+D_i—(n/n_i)^2$……3.1

Phosphorus combine with the vacancy to form a negatively charged phosphrous-vacancy complex by reaction.

$P^+ + V^- \longrightarrow [PV]^-$……3.2

During reaction the phosphorus form the complex near the surface it is reacting with and have high concentration on the surface.

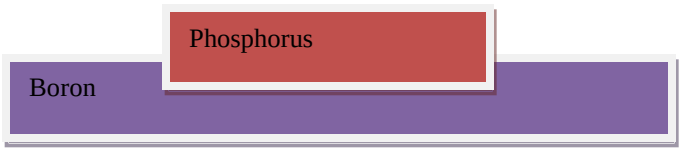

Figure 3.1: Phosphorus diffusion in boron doped silicon.

3.6 Crystal Growth (CZ)

The raw material for PV is provided by the crystal growth method varying with the application of their use as for low power devices we use the CZ material and for high power devices FZ is used because of its more resistivity.

3.6.1 Czochralski Growth

Its name is after that person who devised its growth mechanism and is preferred method because there is no container around the growing crystal. In this method the liquid is under cooled so that the crystal grows down in liquid. A derive mechanism is adjusted to pull the crystal up s fast as it grows.

Figure 3.2: CZ crystal growth.

CHAPTER 4

Experimentation and Results

In this chapter the flow of process and its results will be discussed along with Matlab neural network application. The PV process steps are briefly described with their relevant detail discussed earlier.

Experimentation includes the PV processing, checking of sheet resistance, short circuit current, open circuit voltage and simulation of Matlab program based on the results obtained.

4.1 PV Process Steps:

The process application and output is based on the step by step batch processing of 5”inch sc-silicon wafers that can be described as

1. Selection of boron doped P-type wafers as substrate material for solar cell application with CZ cystal growth and 110 lattice orientation.
2. 1-5 minute KOH dip for surface texturization to help enhance the surface area and reducing the reflectance to absorb more incident rays carrying energy. As surface texturing make pyramids on the surface of substrate and KOH is strong etching agent.
3. RCA-1 cleaning of wafers for 15minutes in the solution constituents as $NH_4OH+H_2O_2$+DI (1:1:5) at 50-70°C.
4. Hydro fluoric acid (HF) dip for 5 minute with diluted in (1:10) with DI water.
5. Emitter deposition- N+ layer on P-Type substrate to get the N type single layer formation on P-substrate. This is the main and most important step in PV process

as a proper recipe for temperature profile and dopant gas concentration is followed to get the required output. This step is any what tells about the reliability and life time of solar cell when put in service.

6. Emitter deposition is followed by step 4 to deglaze the wafers without which the oxide layer will be present on wafer and cell measurements could not be taken.
7. After deglazing the wafer is ready for the sheet resistance measurement by the help of 4-point probe (ResMap).
8. Wafers can now be put in diffusion furnace again for oxide growth and ARC (anti-reflective coating) to help reduce the reflectance which increase their output current.
9. Screen printing is used mostly and here I have used the aluminium back surface field (Al-5072) applied through fine mesh soft baked in recirculating oven for 5 minutes at 220°C and baked at 820-880°C for 120 seconds.
10. After BSF the solar cells are dipped in concentrated HCL for removing residue ash at about 40°C for 1 Hr.
11. Wafers are subjected to ultrasonic cleaning to further cleanse them from BSF ash.
12. Front grid of Ag/Al (4075) is applied through fine mesh and soft baked in air circulating oven at 220°C for 5 minutes.
13. Then solar cells are fired at 760°C for 80-140 seconds in presence of nitrogen.
14. The edge isolation is done by chemically etching the solar cells surface at edges through etching by KOH/NaOH solution.

4.2 Experimentation results

Following are the experimental results including dosing of dopant, time for process,

Temperatue , sheet resistance, open circuit voltage and short circuit current.

Table: 4.1

S#	Time(min)	)	Dopant(ltr)	S-R(Ω/□)	Voltage(v)	Current(A)
1	15	1000	.7	8.25	.49	1.22
2	65	880	.3	27.26	.5	1.81
3	65	880	.3	28.35	.52	1
4	65	880	.3	27.2	.49	1.65
5	45	890	.82	31.67	.41	.88
6	45	890	.82	36.45	.45	1.41
7	45	890	.84	26	.54	1.71
8	35	890	.828	31.47	.49	1.46
9	45	890	.833	30.87	.55	1.55
10	35	890	1.21	23.88	.42	1.02
11	45	890	.8	26.11	.51	1.26
12	45	890	.8	29.5	.47	1.69
13	45	890	.8	27.2	.49	1.6
14	55	895	.8	23.1	.53	1.73
15	55	895	.78	32.06	.48	1.4
16	55	895	.54	23.92	.54	2
17	40	895	.5	31.74	.54	1.74
18	50	895	.5	27.77	.5	1.7
19	55	895	.55	24.65	.53	1.7
20	70	895	.7	22.42	.5	1.71
21	20	900	.82	56.09	.43	1.35
22	10	900	.76	65.5	.49	2
23	10	900	.64	42.31	.52	1.73
24	120	900	.4	20.31	.52	1.78
25	120	900	.4	27.8	.54	2.03
26	10	900	.64	37.36	.48	1.73
27	70	900	1.33	18.4	.46	1.3
28	75	870	.66	31.41	.38	.92
29	20	895	.71	31.61	.49	1.7
30	75	880	.66	28.74	.55	.3
31	20	885	.93	22.1	.5	.76
32	70	860	.54	32.1	.33	.62
33	65	870	.56	25.7	.41	1
34	20	885	.92	22.1	.49	1.31
35	15	1000	.075	23.2	.42	.53
36	15	1000	.1	19.8	.49	.41
37	15	1000	.35	9.68	.47	1.1
38	45	875	1.33	20.48	.48	1.08
39	45	875	1	26.11	.47	.98
40	70	860	.54	29.76	.57	1.24

41	65	870	.56	27.66	.53	1.59
42	65	870	.56	27.05	.54	2.3
43	70	860	.54	37.5	.55	2.1
44	65	880	.56	27.7	.5	1.65
45	70	860	.54	28.3	.53	1.95
46	70	860	.54	28.3	.53	1.96
47	67	860	.47	76.95	.51	1.8
48	67	860	.47	48.8	.52	1.68
49	67	860	.47	32.38	.52	1.6
50	58.05	880	.4	29.85	.5	1.2
51	59	880	.42	21.5	.48	1
52	67	860	.48	32.5	.54	1.95
53	69	880	.39	38.1	.5	1
54	60	880	.44	19.5	.5	1.54
55	60	880	.44	29	.56	2.2
56	15	890	.71	28.2	.56	2
57	25	885	.71	23.5	.56	1.85
58	5	975	.71	21.7	.56	1.9
59	5	975	.71	21.35	.54	2.1
60	5	1000	.71	14.75	.47	1.6
61	5	975	.71	17.55	.54	1.9
62	5	1000	.71	13.6	.53	1.55
63	5	1000	.71	11.5	.52	1.7
64	5	950	.71	30..85	.53	2
65	10	900	.71	35.6	.53	1.4
66	5	950	.71	31.3	.52	2.27
67	5	1000	.71	12.16	.49	1.8
68	5	1000	.71	16.1	.5	1.84
69	5	950	.71	30.35	.52	1.87
70	5	1000	.71	17.1	.53	2.15
71	5	1000	.71	15.65	.48	1.75
72	5	1000	.71	15	.49	1.7
73	10	900	.71	34.79	.51	1.79
74	2	1000	.71	20.7	.5	1.98
75	5	950	.71	29.34	.54	1.8
76	5	950	.71	34.75	.54	2.14
77	5	900	.71	51	.46	1.8
78	5	950	.71	32.86	.42	1.05
79	5	950	.71	34.3	.52	2.06
80	5	950	.71	33	.54	2.15
81	4	965	.71	19.75	.5	1.56
82	4	950	.71	24.5	.48	1.3
83	4	965	.71	25.36	.49	1.45
84	4	975	.71	23.14	.5	1.64
85	5	1000	.5	14.7	.53	1.4

86	**15**	**1000**	**.71**	**5**	**.43**	**.16**
87	**10**	**900**	**1**	**21.4**	**.37**	**.22**
88	**10**	**910**	**1**	**34**	**.32**	**.48**
89	**15**	**1000**	**.45**	**17.5**	**.43**	**1.32**
90	**35**	**890**	**1.5**	**28**	**.51**	**.38**

Here we have first fifty values used for the network training and remaining 40 for checking of the network performance when applied to NN applications.

4.3 Matlab Simulation

These results have been simulated in matlab by forming the neural network and assigning the training/testing sets for network checking.

Here we have used the following commands to create the feed forward error back propagation network

4.3.1 Newff

Create feed-forward backpropagation network

4.3.1.1 Syntax

net = newff(P,T,[S1 S2...S(N-l)],{TF1 TF2...TFNl},

BTF,BLF,PF,IPF,OPF,DDF)

4.3.1.2 Description

newff(P,T,[S1 S2...S(N-l)],{TF1 TF2...TFNl}, BTF,BLF,PF,IPF,OPF,DDF) takes several arguments

4.3.2 sim

Simulate dynamic system

4.3.2.1 Syntax

sim(model,timespan,options,ut);

[t,x,y] = sim(model,timespan,options,ut);

[t,x,y1, y2, ..., yn] = sim(model,timespan,options,ut);

4.3.2.2 Description

The sim command causes the specified Simulink® model to be executed. The model is executed with the data passed to the sim command, which may include parameter values specified in an options structure.

4.3.3 Trian

Train neural network

4.3.3.1 Syntax

[net,tr,Y,E,Pf,Af] = train(net,P,T,Pi,Ai,VV,TV)

4.3.3.2 Description

Train trains a network net according to net.trainFcn and net.trainParam.

4.3.4 Trainlm

Levenberg-Marquardt backpropagation

4.3.4.1 Syntax

[net,TR] = trainlm(net,TR,trainV,valV,testV)

4.3.4.2 Description

Trainlm is a network training function that updates weight and bias values according to Levenberg-Marquardt optimization. Trainlm is often the fastest back propagation algorithm in the toolbox, and is highly recommended as a first-choice supervised algorithm, although it does require more memory than other algorithms.

4.3.5 Traingd

Gradient descent backpropagation.

4.3.5.1 Syntax

[net,TR] = traingd(net,TR,trainV,valV,testV)

4.3.5.2 Description

Traingd is a network training function that updates weight and bias values according to gradient descent.

4.3.6 Program variables

Following are the program variables as defined for simulation:

Table-4.2: Program Variables

Name	Size	Bytes Class
P	3x50	1200 double
P1	1x50	400 double
P2	1x50	400 double
P3	1x50	400 double
T	1x3	24 double
T1	1x50	400 double
T2	1x50	400 double
T3	1x50	400 double
Y	1x50	400 double
Y2	1x50	400 double
Y3	1x50	400 double
YY2	1x40	320 double
YY3	1x40	320 double
ans	1x18	36 char
c1	40x1	320 double

c2	40x1	320 double
c3	40x1	320 double
check_input	40x3	960 double
check_output	40x3	960 double
cont_u	1x1	8 double
data	90x6	4320 double
ind	1x4	32 double
inputs	90x3	2160 double
lim	3x2	48 double
net	1x1	44475 struct
net01	1x1	44475 struct
net1	1x1	44475 struct
net2	1x1	60155 network
net3	1x1	60155 network
outputs	90x3	2160 double
t_end	1x1	8 double
t_init	1x1	8 double
tout	220x1	1760 double
tr	1x1	60820 struct
train_input	50x3	1200 double
train_output	50x3	1200 double
vec	3x4	68 double- sparse

4.3.6 Simulation of Neural networks:

Following are the simulation results of the networks:

4.3.6.1 Simulation #1

This simulation is done with network having logsig function in hidden layer and tansig/purelin in input/output layers with Levenberg-Marquardt learning.

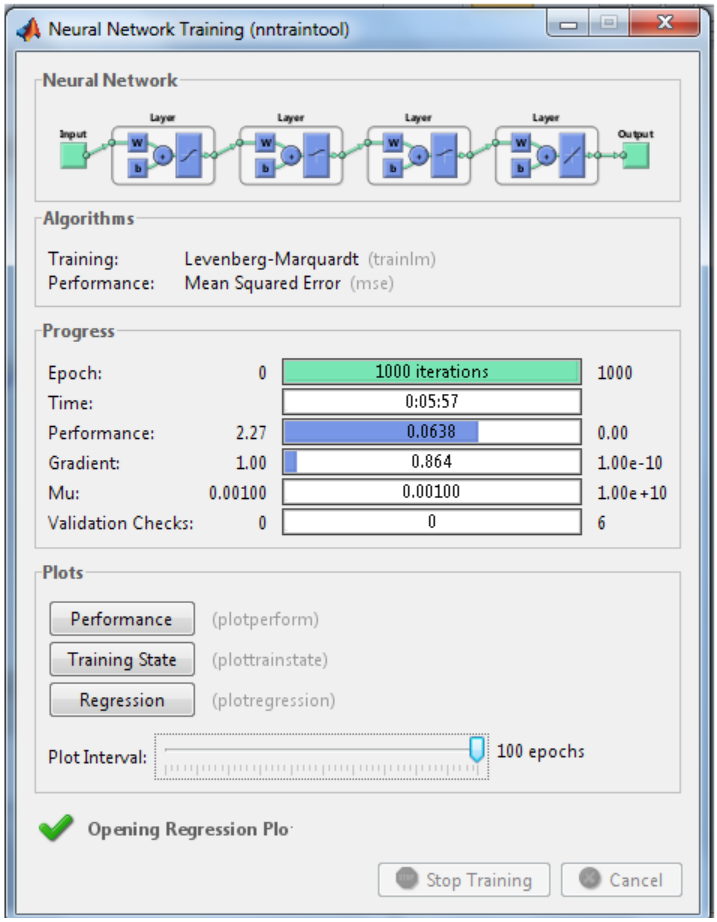

Figure 4.1: Neural Network Training (sim.1)

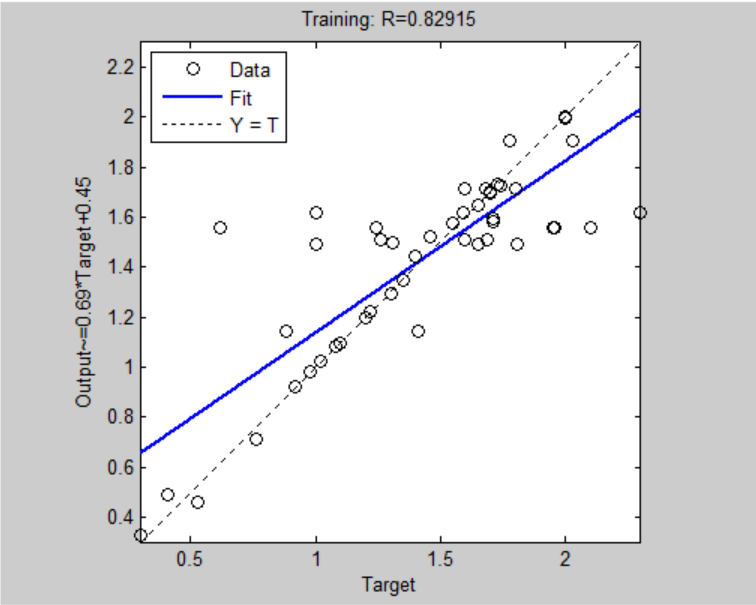

Figure 4.2: Regression of Network (Sim.1)

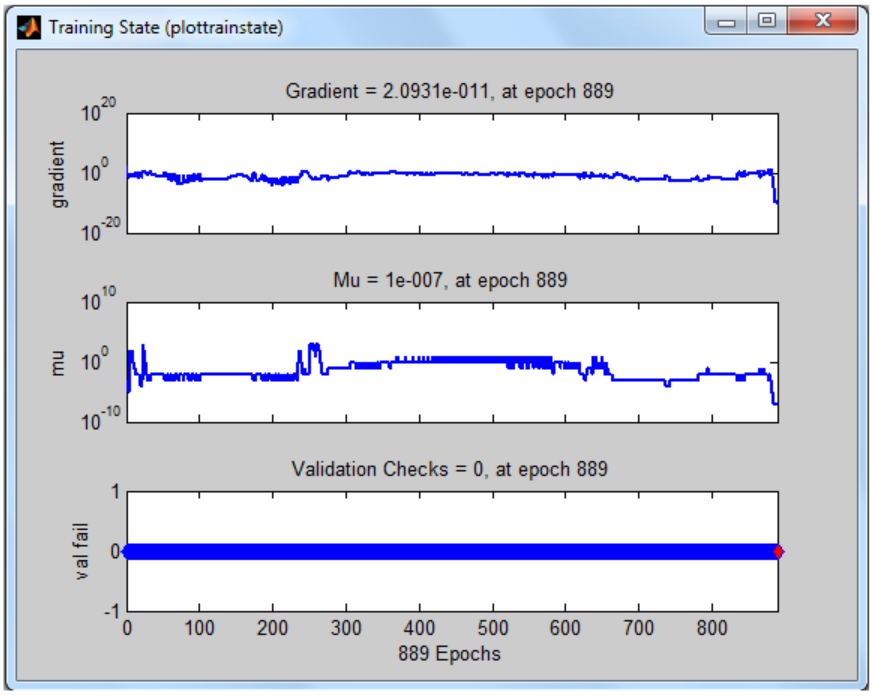

Figure 4.3: Training State of Network (Sim.1)

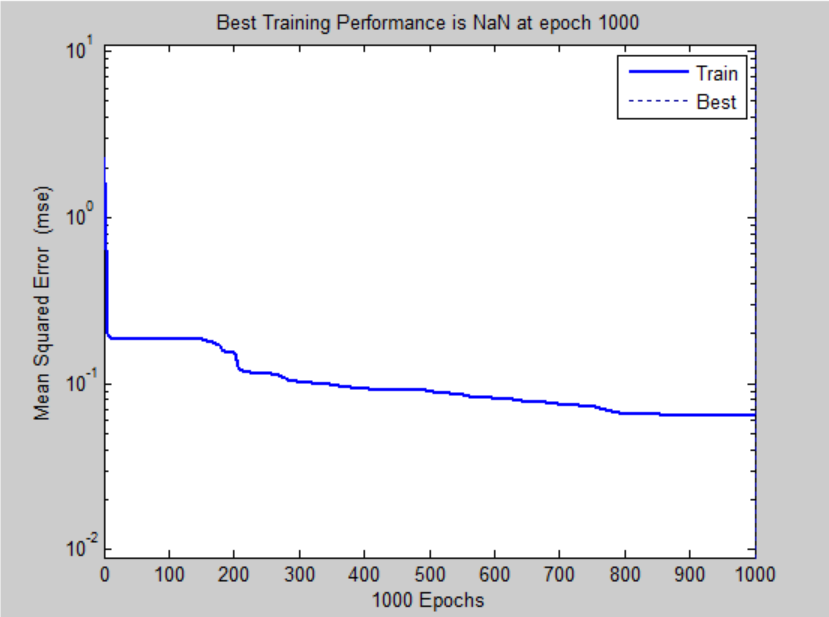

Figure 4.4: Mean Square Error of Network (Sim.1)

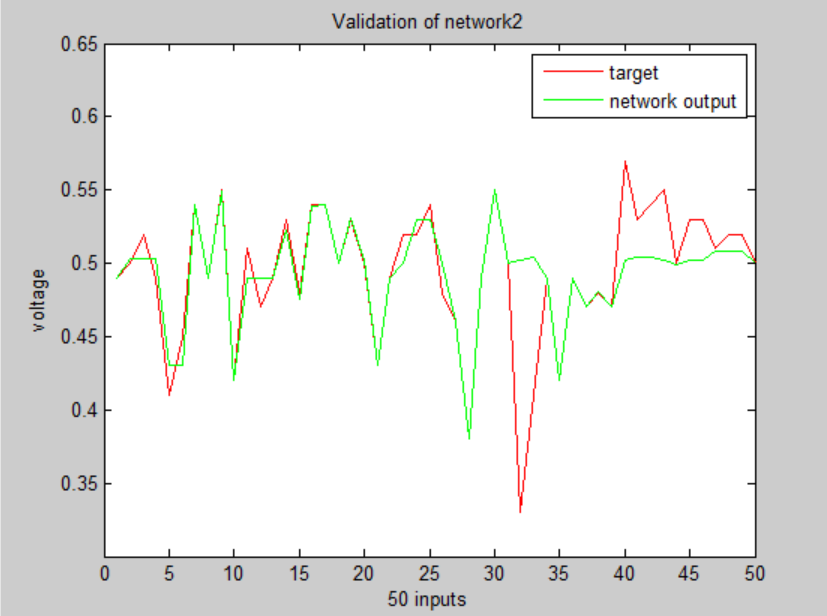

Figure 4.5: Validation of Network against V (Sim.1)

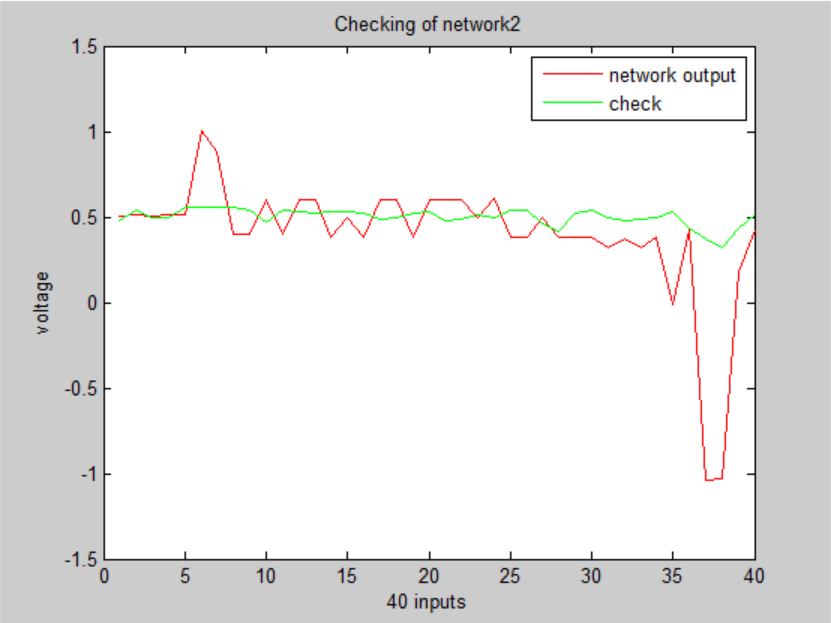

Figure 4.6: Checking of Network against V (Sim.1)

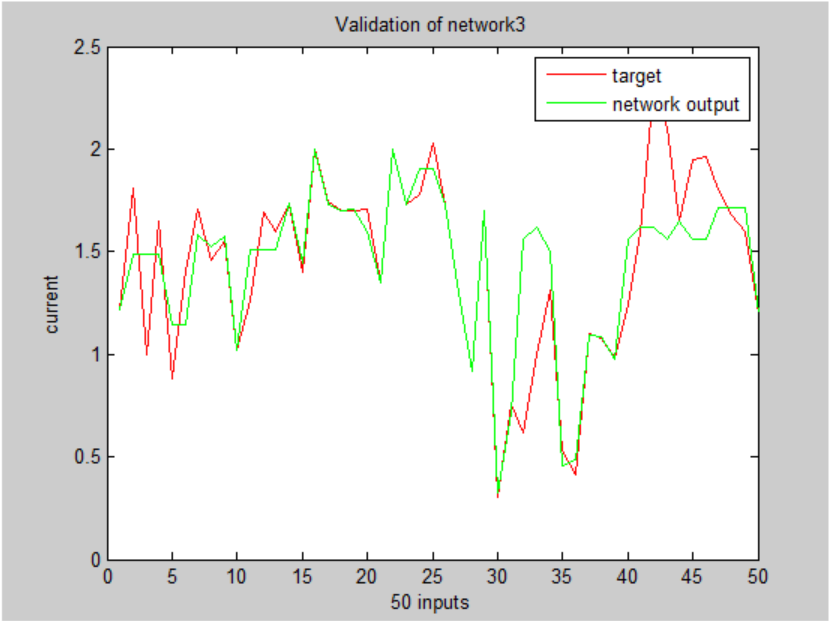

Figure 4.7: Validation of Network against I (Sim.1)

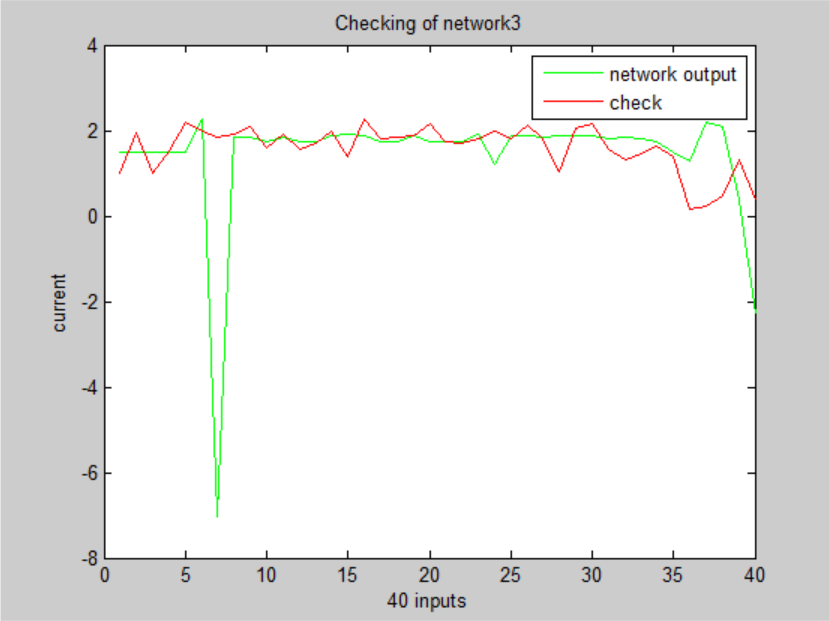

Figure 4.8 :Checking of Network against I (Sim.1)

4.3.6.2 Simulation network#2

This simulation is done with network having tansig function in hidden layer and tansig/purelin in input/output layers with Levenberg-Marquardt

learning.

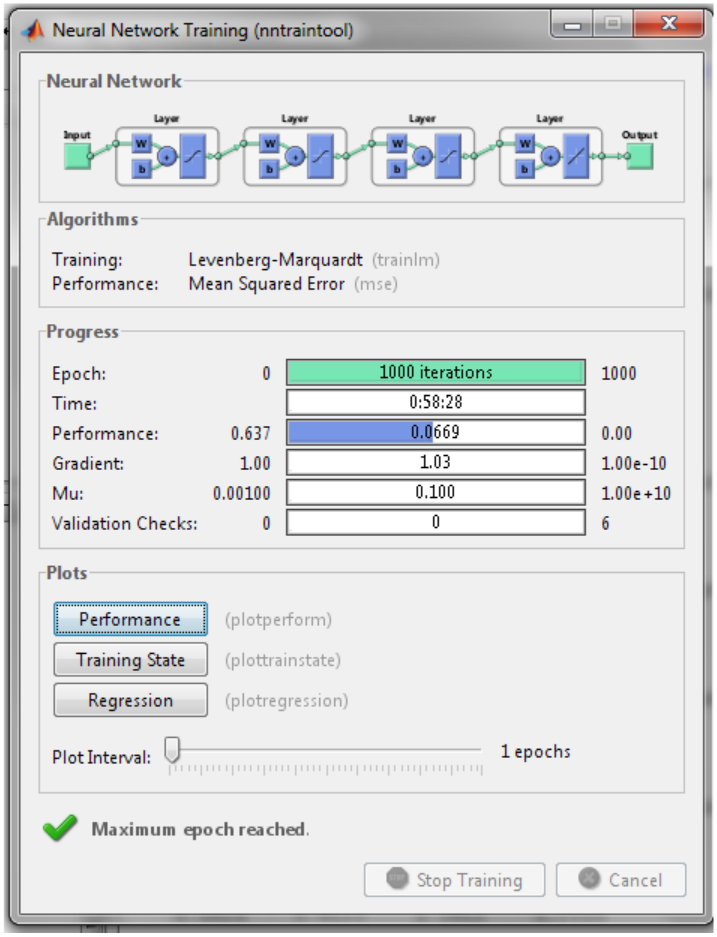

Figure 4.9: Neural Network Training (sim.2)

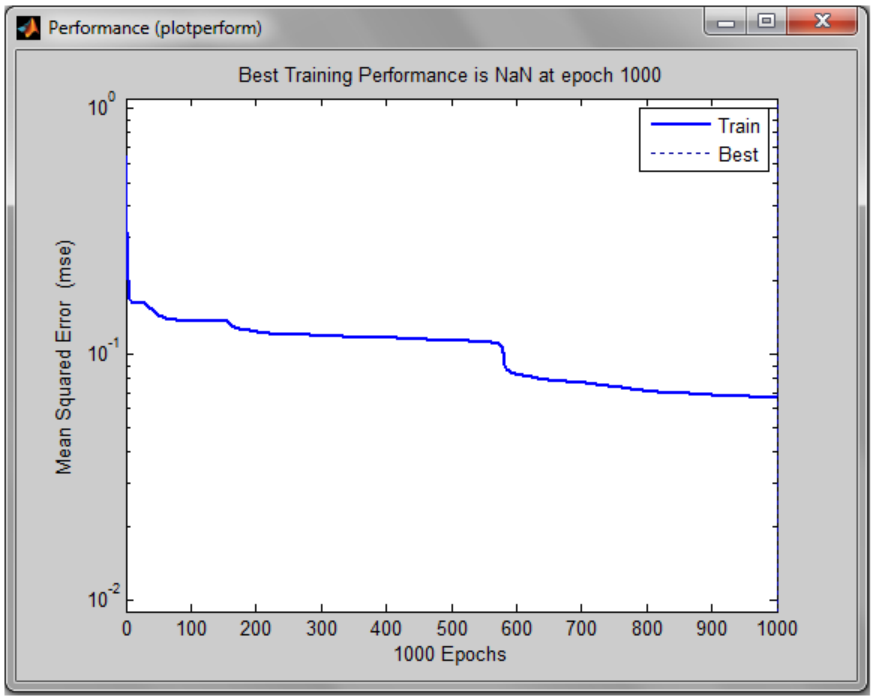

Figure 4.10 : Mean Square Error of Network (Sim.2)

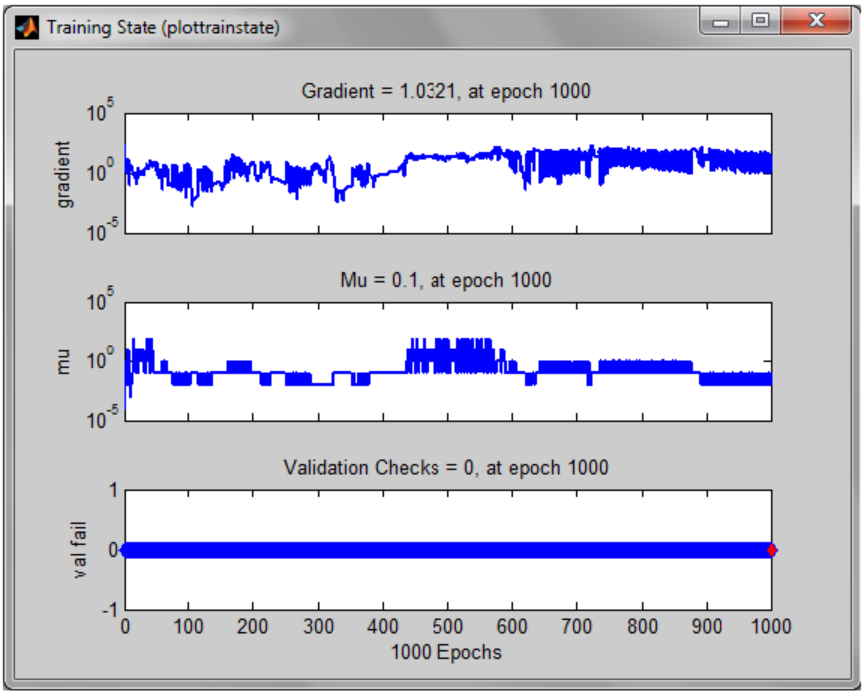

Figure 4.11: Training State of Network (Sim.2)

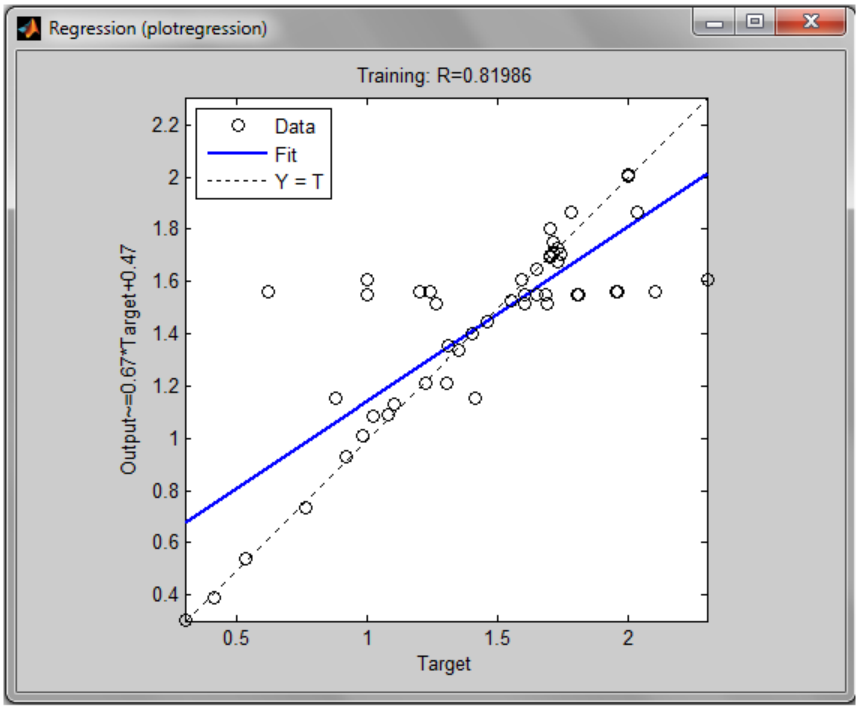

Figure 4.12 : Regression of Network (Sim.2)

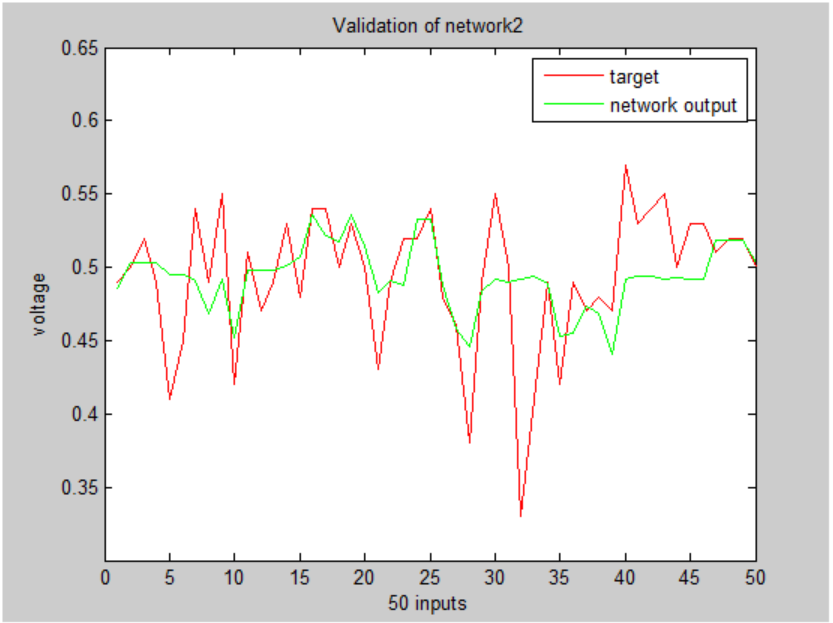

Figure 4.13: Validation of Network against V (Sim.2)

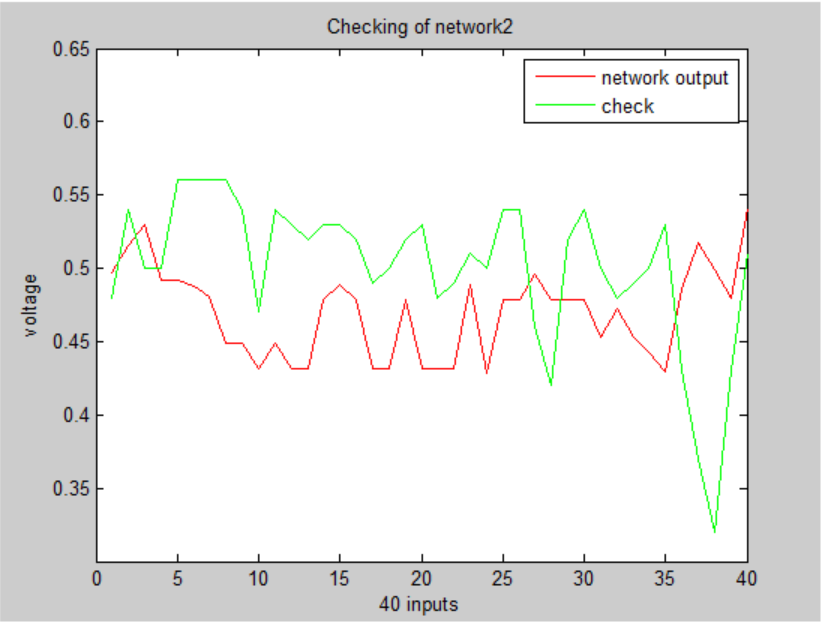

Figure 4.14: Checking of Network against V (Sim.2)

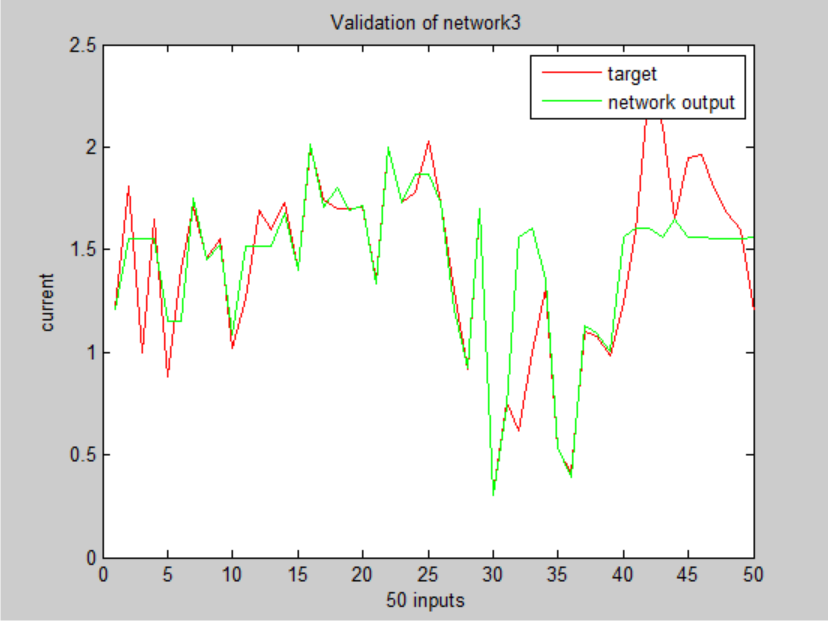

Figure 4.15: Validation of Network against I (Sim.2)

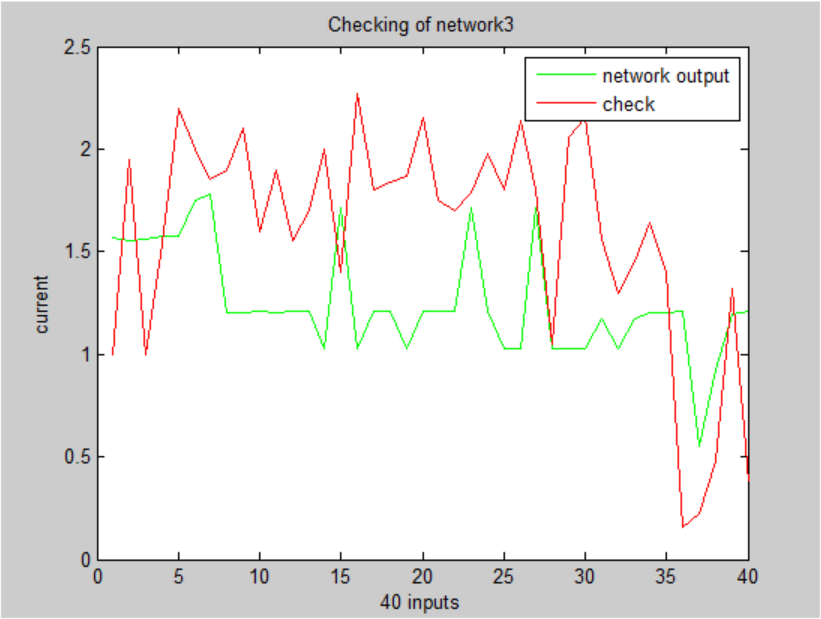

Figure 4.16: Checking of Network against I (Sim.2)

4.3.6.3 Simulation network#3

This simulation is done with network having tansig function in hidden layer and tansig/purelin in input/output layers with Gradient-Descent learning.

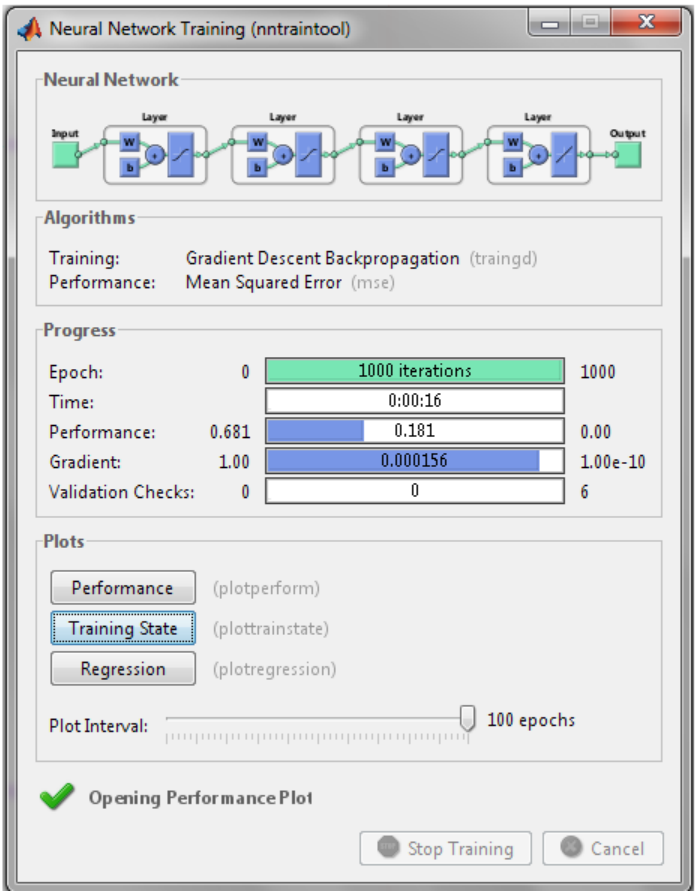

Figure 4.17 : Neural Network Training (sim.3)

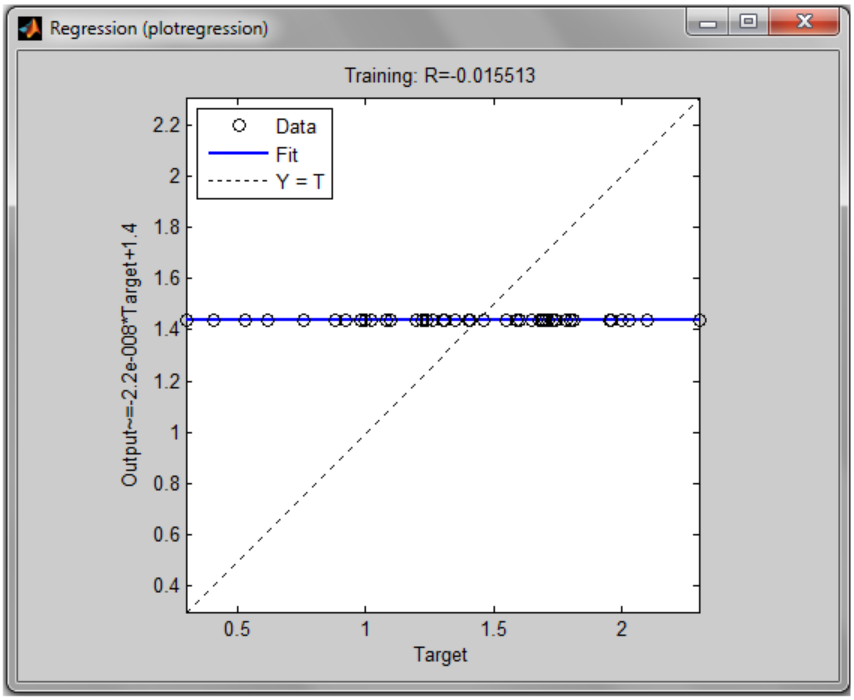

Figure 4.18: Regression of Network (Sim.3)

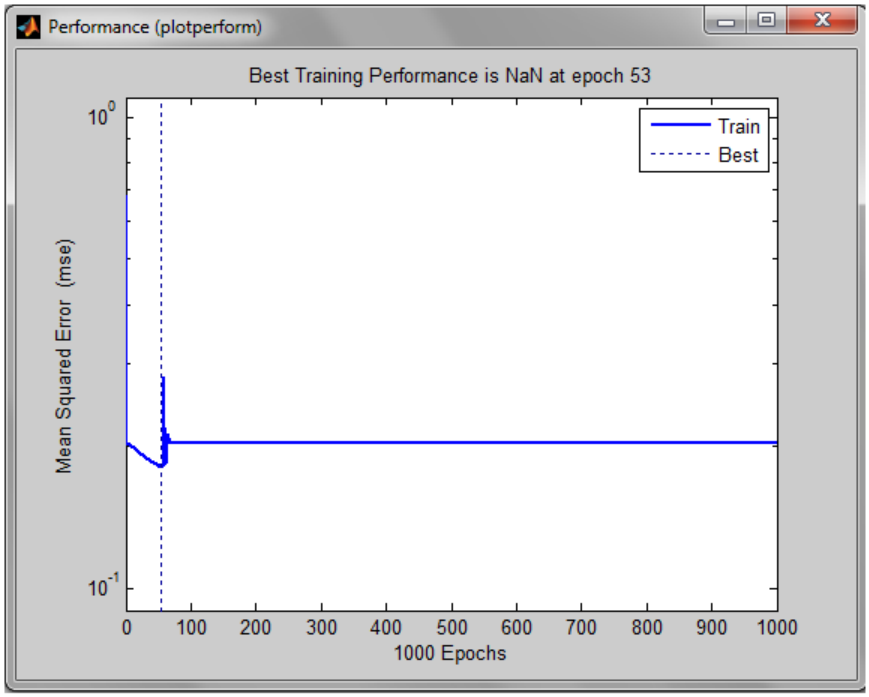

Figure 4.19: Mean Square Error of Network (Sim.3)

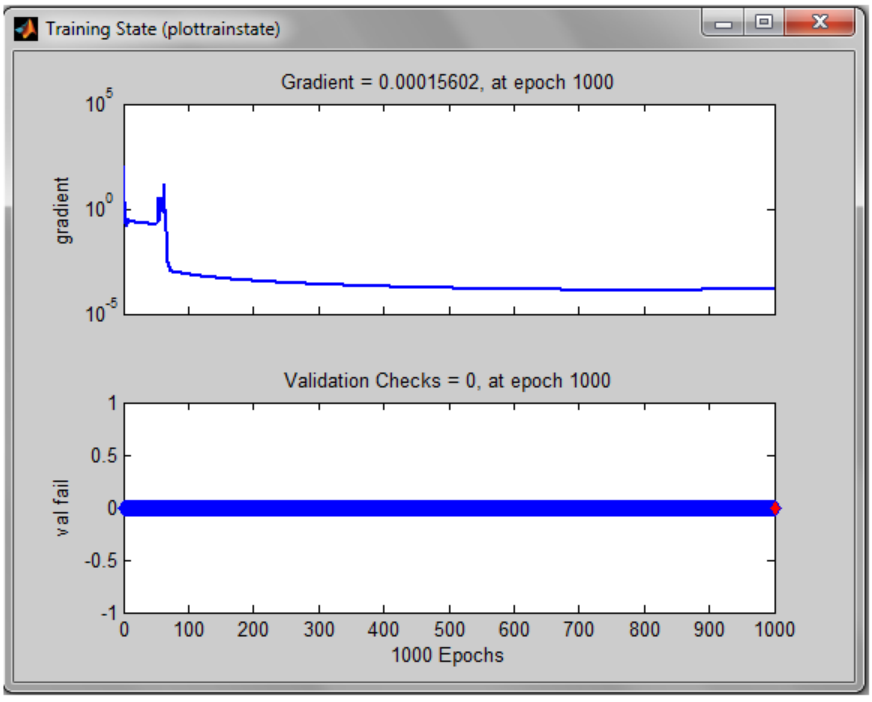

Figure 4.20: Training State of Network (Sim.3)

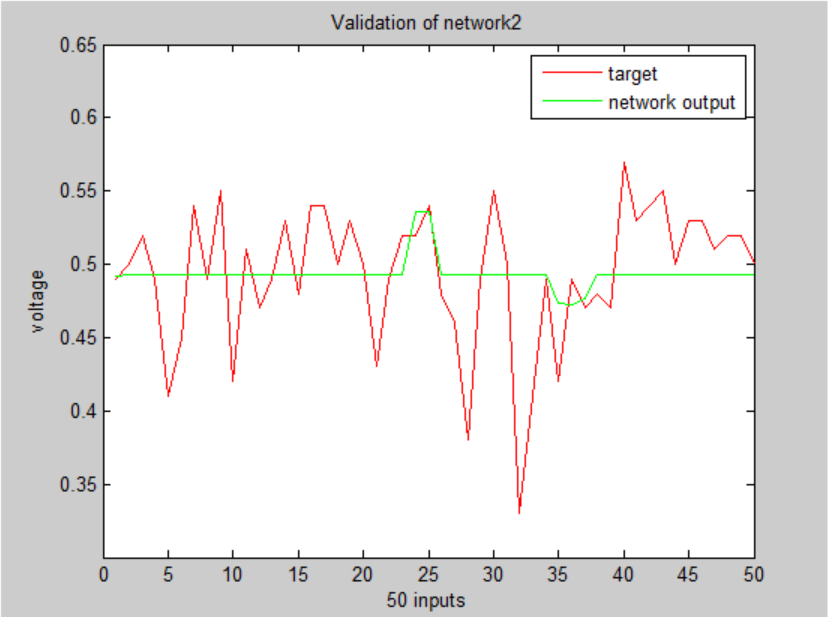

Figure 4.21: Validation of Network against V (Sim.3)

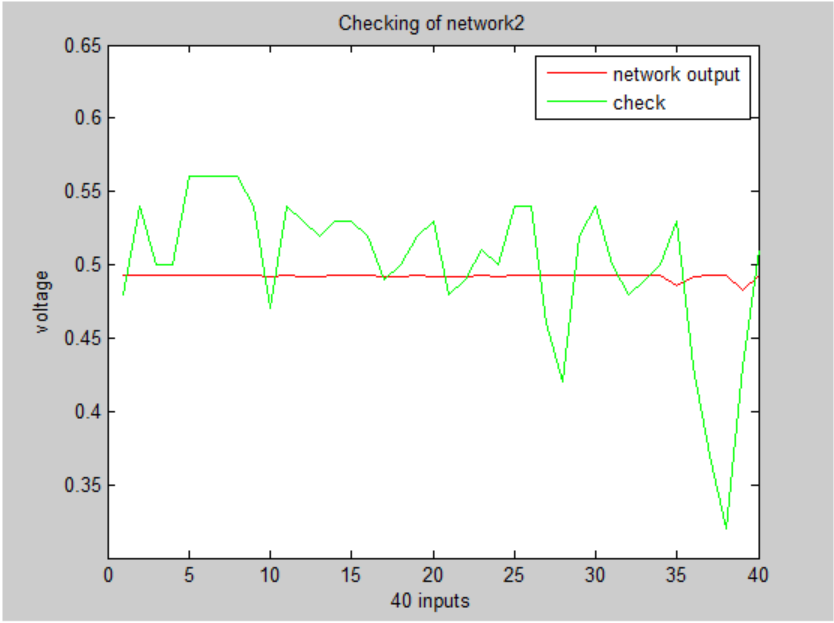

Figure 4.22: Checking of Network against V (Sim.3)

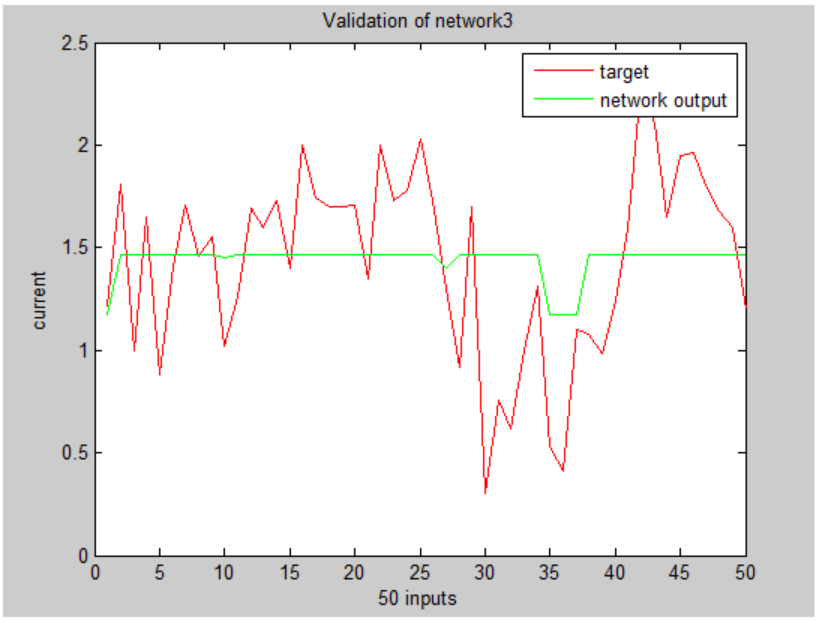

Figure 4.23 : Checking of Network against I (Sim.3)

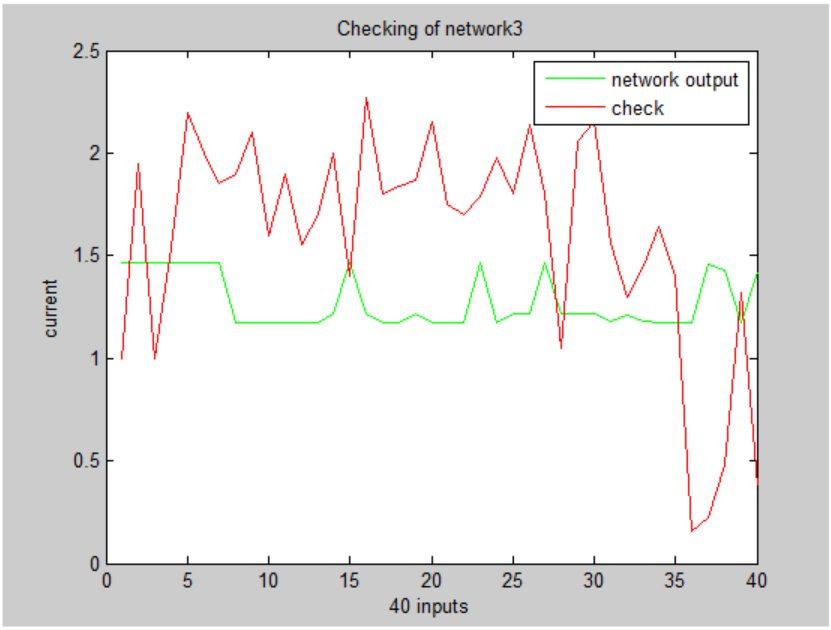

Figure 4.24: Checking of Network against I (Sim.3)

4.4 Matlab Coding:

Matlab source coding is given in annexure with the title for each simulation run as:

- Simulation#1 (Sim.1)
- Simulation#2 (Sim.2)
- Simulation#3 Sim.3)

With the help of these simulations it is evident that network gives nearly same results as by actual experimentation performed which serve the purpose of simulation.

4.5 Neural Networks Characteristics and Outcomes:

With the use of experimental data the network has been trained that gives the same output as we expect from the actual experimentation.

Table: 4.3 - NN simulation characteristics.

Characteristic.	Net #1	Net#2	Net#3
Training.	LM	LM	GD
Performance.	MSE	MSE	MSE
Epoch.	1000	1000	1000
Time (h:m:s)	0:54:22	0:05:57	0:0:16
Gradient.	2.2	2.09e-11	.000156
Regression.	.545	.827	.0155
No. of Layers.	4	4	4
Transfer Functions .	Tansig,tansig,tansig,purlin.	Tansig,logsig,logsig,purlin.	Tansig,tansig,tansig,purlin.

4.6 ARC Application and Increment in I &V:

- By using open tube diffusion furnace and oxide growth method of ARC we produced solar cells that are producing same output as any of the commercially available sc-silicon PV cells.
- With ARC application after emitter deposition following resultant increase is seen in the current and voltages of solar cells.

Table: 4.4- ARC application and results.

Samples	Current(mA)	Current(mA)	24% - increase	Voltage(v)	Voltage(v)	17% - increase
1	980	1220	19.7	.41	.49	16.3
2	1350	1810	25.4	.42	.5	16.0
3	780	1000	22.0	.45	.52	13.5
4	1320	1650	20.0	.42	.49	14.3
5	640	880	27.3	.36	.41	12.2
6	1130	1410	19.9	.37	.45	17.8
7	1210	1710	29.2	.46	.54	14.8
8	980	1460	32.9	.39	.49	20.4
9	1120	1550	27.7	.45	.55	18.2

10	**780**	**1020**	**23.5**	**.31**	**.42**	**26.2**

CHAPTER 5

Futuristic

This thesis gives us the introduction about the photovoltaic processing and the results that can be used to form neural network for result prediction prior to experimentation.

Following are the things that can be done to make things improved by implementation of the neural network tools with the resulting experiments:

- Other parameters of process can be included like cell efficiency and its prediction.
- Neural simulation is widely used in semiconductor application but for PV its introduction would appreciably increase the yield.
- End product can be enhanced through avoiding breakage of wafers and data can be incorporated with operator wise simulation with each batch processing steps.
- Neural application of PV process development can be implemented as package to the semiconductor industries having PV processing or single layer process application i.e. diffusion control, temperature profile and recipe synthesis.
- Solar cells are now becoming feasible with respect to cost as the energy crises is growing and it can help to implement the new products that may enhance its yield.
- Thin >200micron solar cells reduce the cost of material and those can be implemented with validation of experimentation as having same efficiency as thick cells with NN application to stop their frequent breakage.

So by the implementation of these results we can rightly predict the improvement in PV process and its further development.

CONCLUSION

This study is helpful in understanding the photovoltaic process and how we can make solar cells. It is also providing the flow of batch processing mechanism that is shown during working in FAB for semiconductor applications and provides us with the basic learning of clean room work environment. In this work some of the equipment their usage for PV processing and proper process development is described.

This result oriented work is implemented through the use of simulation of neural network to get the predicted results from the data set obtained from experimentation. So this piece of work provide with the photovoltaic process development and its application in implementing the neural simulator successfully.

In this process development work some of the techniques have been highlighted that tells us about the constant improvement is must for any processing industry i.e. BSF-Al application using 5072 Al-paste for the back contact of solar cell we can reduce the resistance in contact by removing the residual ash that sticks to it in firing process. This removal of ask from back surface field with concentrated HCL help us to provide with good contact of each solar cell when put in PV module.

Surface texturing rate vary with the concentration of KOH and time given for the etching process. But with lattice orientation and temperature profiling we get optimum etch rate with respect to cell output in terms of efficiency for each process line as unique.

Results obtained from experimentation can be used to model each step of process as separate optimizer to enhance the overall performance of work as sheet resistance gives good tracking of solar process specially relating to diffusion.

In this work the neural network have been trained using supervised learning with all the targets given in training set and their validation is further checked by the introduction of checking network with targets from the sample, however we can also trace back the inverse of it and can get inputs with targets defined. This can be of great help in synthesis of recipe for PV processing related to diffusion, ARC and firing of front and back grid connections, as with currently developed network we can trace the diffusion optimization time and dopant concentration with temperature profiling.

So the trained neural network is of great application for photovoltaic processing and can be considered as a package for this processing application.

REFERENCES

[1] Deionized (DI) Water Filtration, “Field Applications HCP-13e”, available on-line at http://www.pall.com/pdf/HCP-13e.pdf, 2010.

[2] SW Jones ,Diffusion in Silicon, “chapter on Diffusion in Silicon”, available on-line at http://www.icknowledge.com/misc_technology/Diffusion.pdf, 2008.

[3] Chang, J.J., “Concentration-dependent diffusion of boron and phosphorus in silicon,” *Electronic Devices*, vol. 10, no.6, pp.357-359, 1963.

[4] Thin Film Deposition , “Four-Point Probe Operation”, available on-line at http://www.utdallas.edu/research/cleanroom/manuals/documents/4pointFinal.pdf,2004.

[5] B. Vallejo , M. González-Mañas , J. Martínez-López and M.A. Caballero, “ On the texturization of monocrystalline silicon with sodium carbonate solutions”, *Solar Energy*,vol. 81, no. 5, pp. 565-569, 2007.

[6] Nijs, J.F.; Szlufcik, J.; Poortmans, J.; Sivoththaman, S.; Mertens, R.P “ Advanced manufacturing concepts for crystalline silicon solar cells,” *Electron Devices*,vol.46,no.10,pp.1948-1969, 1999.

[7] Meier, D.L.; Hwang, J.-M.; Campbell, R.B.; , “The effect of doping density and injection level on minority-carrier lifetime as applied to bifacial dendritic web silicon solar cells,” *Electron Devices*,vol.35,no.1,pp.70-79, 1988.

[8] Lee-Ing Tong ,Wei-I Lee and Chao-Ton Su,“ Using a neural network-based approach to predict the wafer yield in integrated circuit manufacturing,” *IEEE Transactions on Components, Packaging, and Manufacturing Technology*, vol. 20,no.4,pp.288-294,August 2002.

[9] Huang, Y.L., Edgar, T.F., Himmelblau , D.M. and Trachtenberg, I. ,"Constructing a reliable neural network model for a plasma etching process using limited experimental data.," *IEEE transaction on semiconductor manufacturing*. Vol. 7 , no. 3, pp. 333 – 344,1994.

[10] Seung-Soo Han., Li Cai., May, G.S., Rohatgi, A., "Modeling the growth of PECVD silicon nitride films for solar cell applications using neural networks.," *IEEE transaction on semiconductor manufacturing*,vol.9,no.3,pp.303-311,1996.

[11] Kim, B.; Kim, S.; Kim, K.; , "Use of neural network to characterize temperature effects on refractive property of silicon nitride film deposited by PECVD," in *Proc. 30th IEEE International Conference on Plasma Science, 2003. ICOPS 2003.*

[12] Han, S.S.; Ceiler, M.; Bidstrup, S.A.; Kohl, P.; May, G.; , "Modeling the properties of PECVD silicon dioxide films using optimized back-propagation neural networks. ," *IEEE Transactions on Components, Packaging, and Manufacturing Technology*, Vol. 17 ,no.2,pp.174-182,1994.

[13] Simulator software tool, "An Object-Oriented Neural Network Simulator for Semiconductor Manufacturing Applications", available on-line at http://users.ece.gatech.edu/~gmay/SCI04.pdf, 2004.

[14] Chinmoy B. Bose; Herbert A. Lord , "Neural network models in wafer fabrication," in *Proc. SPIE Application of Artificial Neural Networks. IV , September 1993,pp.521-530.*

[15] Sheoran, Manav ; Upadhyaya, A. D. ; Rounsaville, Brian ; Kim, Dong Seop ; Rohatgi, Ajeet ; Narayanan, S.,"Investigation of the Effect of Resistivity and Thickness on the Performance of Cast Multicrystalline Silicon Solar Cells," in *Proc.* 4th World

Conference on Photovoltaic Energy Conversion; Hawaii, USA. http://hdl.handle.net/1853/25923, 2006.

[16] Duran, E.; Piliougine, M.; Sidrach-de-Cardona, M.; Galan, J.; Andujar, J.M.; , "Different methods to obtain the I–V curve of PV modules: A review," in *Proc.33rd IEEE photovoltaic specialists conference, PVSC, San Diego, CA, USA, 2008.*

[17] Barnett, Allen; Wang, Xiaoting; Waite, Nick; Murcia, Paola; Honsberg, Christiana; Kirkpatrick, Doug; Laubacher, Dan; Kiamilev, Fouad; Goossen, Keith; Wanlass, Mark; Steiner, Myles; Schwartz, Richard; Gray, Jeff; Gray, Allen; Sharps, Paul; Emery, Keith; Kazmerski, Larry; "Initial test bed for Very High Efficiency Solar Cell," in *Proc.33rd IEEE photovoltaic specialists conference, PVSC, San Diego, CA, USA, 2008.*

[18] Lautenschlager, H.; Lutz, F.; Schetter, C.; Schubert, U.; Schindler, R.; "MC SILICON SOLAR CELLS WITH > 17 % EFFICIENCY," in *Proc.26th IEEE conference of Photovoltaic Specialists*,Anaheim,CA,USA,1997.

[19] W.E.Beadle, J.C.C.Tsai, R.D.Plummer ; "Chemical Etchants for silicon Defects:Table-5.2," *in Chemical Recipes from Quick Reference Manual for Silicon Integrated Circuit Technology John Wiley & Sons* ,pp.5-12, *NY, USA, 2008.*

ABBREVIATIONS

PECVD: plasma enhanced chemical vapor deposition.

PV: photovoltaic.

MC: Multi crystalline.

SC: Single crystal.

FZ: Float zone.

CZ: Czochralski.

VHESC: Very high efficiency solar cells.

CVD: Chemical vapor deposition.

SEM: Scanning electron microscope.

ANN: Artificial neural network.

BPNN: Back propogation neural network.

ART: Adaption resonance theory.

PCD: Photoconductive decay.

Annexure

Matlab Codes:

Simulation#1 (Sim.1)

```
clear all
close all
load icdata4


c1=check_output(:,1) %col 4
c2=check_output(:,2) %col 5
c3=check_output(:,3) %col 6

net2 = newff(lim ,[30 15 10 1],{'tansig' 'logsig' 'logsig' 'purelin'});
net2 = train(net2,P,T2);
Y2=sim(net2,P)

figure
plot(T2,'r')
hold on
plot(Y2,'g')
title('Validation of network2')
xlabel('50 inputs')
ylabel('voltage')
legend('target', 'network output')

figure
YY2=sim(net2,check_input')
plot(YY2,'r')
hold on
plot(c2,'g')
title('Checking of network2')
xlabel('40 inputs')
ylabel('voltage')
legend('network output', 'check')

net3 = newff(lim ,[30 15 10  1],{'tansig' 'logsig' 'logsig'
'purelin'});
net3=train(net3,P,T3)
Y3=sim(net3,P)

figure
plot(T3,'r')
hold on
plot(Y3,'g')
title('Validation of network3')
xlabel('50 inputs')
ylabel('current')
legend('target', 'network output')
```

```
figure
YY3=sim(net3,check_input')
plot(YY3,'g')
hold on
plot(c3',’r')
title('Checking of network3')
xlabel('40 inputs')
ylabel('current')
legend('network output', 'check')

save icdata4
```

Simulation#2 (Sim.2)

```
clear all
close all
load icdata4


c1=check_output(:,1) %col 4
c2=check_output(:,2) %col 5
c3=check_output(:,3) %col 6

net2 = newff(lim ,[30 15 10 1],{'tansig' 'tansig' 'tansig' 'purelin'});
net2 = train(net2,P,T2);
Y2=sim(net2,P)

figure
plot(T2,'r')
hold on
plot(Y2,'g')
title('Validation of network2')
xlabel('50 inputs')
ylabel('voltage')
legend('target', 'network output')

figure
YY2=sim(net2,check_input')
plot(YY2,'r')
hold on
plot(c2,'g')
title('Checking of network2')
xlabel('40 inputs')
ylabel('voltage')
legend('network output', 'check')

net3 = newff(lim ,[30 15 10  1],{'tansig' 'tansig' 'tansig'
'purelin'});
net3=train(net3,P,T3)
Y3=sim(net3,P)

figure
```

```
plot(T3,'r')
hold on
plot(Y3,'g')
title('Validation of network3')
xlabel('50 inputs')
ylabel('current')
legend('target', 'network output')

figure
YY3=sim(net3,check_input')
plot(YY3,'g')
hold on
plot(c3','r')
title('Checking of network3')
xlabel('40 inputs')
ylabel('current')
legend('network output', 'check')

save icdata4
```

Simulation#3 (Sim.3)

```
clear all
close all
load icdata4


c1=check_output(:,1)
c2=check_output(:,2)
c3=check_output(:,3)

net2 = newff(lim ,[30 15 10 1],{'tansig' 'tansig' 'tansig'
'purelin'},'traingd');
[net2,tr,Y] = train(net2,P,T2);
%net2 = traingd(net2,P,Y);
Y2=sim(net2,P)

figure
plot(T2,'r')
hold on
plot(Y2,'g')
title('Validation of network2')
xlabel('50 inputs')
ylabel('voltage')
legend('target', 'network output')

figure
YY2=sim(net2,check_input')
plot(YY2,'r')
```

```
hold on
plot(c2,'g')
title('Checking of network2')
xlabel('40 inputs')
ylabel('voltage')
legend('network output', 'check')

net3 = newff(lim ,[50 25 15  1],{'tansig' 'tansig' 'tansig'  'purelin'
},'traingd');
[net3,tr,Y3] = train(net3,P,T3);
%net3=traingd(net3,P,T3)
Y3=sim(net3,P)

figure
plot(T3,'r')
hold on
plot(Y3,'g')
title('Validation of network3')
xlabel('50 inputs')
ylabel('current')
legend('target', 'network output')

figure
YY3=sim(net3,check_input')
plot(YY3,'g')
hold on
plot(c3','r')
title('Checking of network3')
xlabel('40 inputs')
ylabel('current')
legend('network output', 'check')

save icdata4
```